Methodology for Assessing Retrofitted Hydrogen Combustion and Fuel Cell Aircraft Environmental Impacts

Khaled Alsamri,* Jessica De la Cruz,† Melody Emmanouilidi,† Jacqueline Huynh,‡ and Jack Brouwer§
University of California Irvine, Irvine, California 92697

https://doi.org/10.2514/1.B39405

Hydrogen (H_2) combustion and solid oxide fuel cells (SOFCs) can potentially reduce aviation-produced greenhouse gas emissions compared to kerosene propulsion. This paper outlines a methodology for evaluating performance and emission tradeoffs when retrofitting conventional kerosene-powered aircraft with lower-emission H_2 combustion and SOFC hybrid alternatives. The proposed framework presents a constant-range approach for designing liquid hydrogen fuel tanks, considering insulation, sizing, center of gravity, and power constraints. A lifecycle assessment evaluates greenhouse gas emissions and contrail formation effects for carbon footprint mitigation, while a cost analysis examines retrofit implementation consequences. A Cessna Citation 560XLS+ case study shows a 5% mass decrease for H_2 combustion and a 0.4% mass decrease for the SOFC hybrid, at the tradeoff of removing three passengers. The lifecycle analysis of green hydrogen in aviation reveals a significant reduction in CO_2 emissions for H_2 combustion and SOFC systems, except for natural-gas-produced H_2 combustion, when compared to Jet-A fuel. However, this environmental benefit is contrasted by an increase in fuel cost per passenger-km for green H_2 combustion and a rise for natural-gas-produced H_2 SOFC compared to kerosene. The results suggest that retrofitting aircraft with alternative fuels could lower carbon emissions, noting the economic and passenger capacity tradeoffs.

Nomenclature

$C_{p,\text{Air}}$	=	specific heat capacity of air
d	=	height of the spherical head
d_o	=	radius of inner tank
d_1	=	width of spherical head
$EI(X)$	=	emission index of species X
e_{weld}	=	weld efficiency
G	=	mixing line slope
g	=	acceleration due to gravity on Earth
h	=	cruising altitude
h_{conv}	=	convective heat transfer coefficient
h_f	=	heat energy available per unit weight of fuel
K	=	geometrical constant
K_{ins}	=	thermal conductivity of insulation
k	=	thermal conductivity of the material
L	=	length of the cylindrical part of tank
L_{cyl}	=	length of cylinder
L/D	=	lift-to-drag ratio
LHV_{fuel}	=	lower heat value of fuel
M_{boiloff}	=	mass boiloff
M_H	=	mass of hydrogen
MAC	=	mean aerodynamic chord
$m_{\text{filledcapsule}}$	=	mass of filled capsule
m_t	=	mass of tank
$\dot{m}$	=	mass flow rate
$\dot{m}_{\text{air}}$	=	mass flow rate of air
$\dot{m}_{\text{fuel}}$	=	mass flow rate of fuel
$\dot{m}_{H_2}$	=	mass flow rate of hydrogen
$\dot{m}_{H_2O}$	=	mass flow rate of water
$\dot{m}_{\text{steam}}$	=	mass flow rate of steam
Nu_D	=	Nusselt number
P	=	pressure
P_a	=	ambient pressure at altitude
P_{des}	=	pressure for hydrogen storage
Pr	=	Prandtl number
Q	=	heat transfer rate
q	=	heat loss
R	=	range
Re_D	=	Reynolds number
r	=	radius
r_{ins}	=	radius of insulation
r_1	=	radius of inner vessel
r_2	=	radius of outer shell
T	=	temperature
T_{atm}	=	atmosphere temperature surrounding the cylinder
T_i	=	inside temperature
T_o	=	outside temperature
t_w	=	wall thickness
t_{wh}	=	wall hemisphere thickness
V_i	=	excess volume
V_{out}	=	volume out
V_{system}	=	volume of tank system
V_t	=	tank volume
W_{fuel}	=	fuel weight
W_{to}	=	maximum takeoff weight
ε	=	emissivity of the surface
ϵ_{H_2O}	=	molar mass of water over mass of dry air
η_{overall}	=	overall engine efficiency
λ_{cabin}	=	tank sizing cabin constraints
λ_{tank}	=	total length of tank
λ_t	=	tank sizing constraints
ρ	=	density
σ_a	=	tensile strength of material for cryogenic tank
τ_{allow}	=	allowable shear stress

Presented as Paper 2023-1954 at the 2023 AIAA Science and Technology Forum and Exposition (AIAA SciTech Forum), National Harbor, MD, January 23–27, 2023; received 7 October 2023; revision received 26 February 2024; accepted for publication 9 March 2024; published online 3 April 2024.

*Graduate Student Researcher, Department of Mechanical and Aerospace Engineering, 4200 Engineering Gateway; kalsamri@uci.edu. Student Member AIAA (Corresponding Author).

†Graduate Student Researcher, Department of Mechanical and Aerospace Engineering, 4200 Engineering Gateway. Student Member AIAA.

‡Assistant Professor, Department of Mechanical and Aerospace Engineering, 4200 Engineering Gateway. Member AIAA.

§Director of Advanced Power and Energy Program, Department of Mechanical and Aerospace Engineering, 4200 Engineering Gateway. Member AIAA.

σ	=	Stefan–Boltzmann constant
$()_{eq}$	=	equivalent
$()_f$	=	property for fuel
$()_{H_2}$	=	property for hydrogen
$()_h$	=	property at altitude
$()_{st}$	=	property at standard temperature
$()_t$	=	property for tank
$()_t$	=	property for tank
$()^*$	=	per segment

I. Introduction

AS AIRLINE traffic is forecasted to increase by approximately 4% annually from 2022 to 2040, the environmental impact and pollution levels in the vicinity of airports have escalated as pressing concerns [1]. To meet the ambitious objective of emission reduction, simply enhancing traditional fossil-fuel-based aviation technologies has been deemed insufficient. Consequently, the exploration and integration of alternative fuels has become a focal point in both academic research and industry initiatives. The scope of current academic inquiry spans a broad spectrum of renewable energy sources, with particular emphasis on battery-electric, solar energy, biomass-derived fuels, and, most notably, hydrogen. The aviation industry's move toward electrification, utilizing battery-based energy sources, offers a promising path to further reduce environmental impacts. However, the gravimetric energy density of batteries represents the primary challenge. For commuter aircraft applications to be viable, pack-level specific energies need to exceed 1200–2000 W·h/kg, which is several times higher than that of current leading lithium-ion batteries [2]. Despite technological advancements, existing battery solutions have not yet met the specific energy density requirements crucial for lightweight components in electric aircraft. As a result, projections suggest that battery-powered aircraft will become practically viable for subregional travel by 2035 [3]. Building on the concept of electrification, the integration of hydrogen fuel cells into hybrid systems emerges as a highly promising development. This approach combines the high energy density of hydrogen fuel cells with the instantaneous power supply of batteries, aiming to address the limitations of each technology when used in isolation. As proposed by Adler and Martins, hybrid systems that leverage the unique strengths of multiple power sources, including hydrogen fuel cells, can significantly enhance efficiency, endurance, and other critical performance metrics [4]. Such hybrid configurations, by synergistically combining different energy sources, present a robust solution to overcome the challenges faced by single-source systems. The potential of hydrogen fuel cells, varying according to the technology employed, underscores their pivotal role in advancing next-generation aviation fuel systems [5].

Solar energy, despite its significant potential as delineated in the study on technological development trends in solar-powered aircraft systems [6], faces critical challenges. These include low energy conversion efficiency and high costs associated with current technologies, which hinder its broader adoption and implementation in aviation and other sectors. One critical challenge is its application in commercial aviation; the current state of solar technology renders it nearly impossible for solar energy alone to power commercial aircraft due to constraints in energy conversion efficiency and the substantial power requirements of larger planes. Biomass energy offers a carbon-neutral alternative for fuel. Yet, its path from biomass to energy forms like liquid hydrogen (LH_2) is marked by complex, energy-heavy processes. These challenges are compounded by environmental concerns and high conversion costs. Moreover, as Wang et al. [7] discuss, bio-aviation fuels face hurdles in technology development, certification, and distribution. The energy-intensive nature of converting lipids and carbohydrates from biomass into aviation fuel pinpoints critical limitations: the high production costs and environmental impacts. Hydrogen energy emerges as a promising candidate within the renewable energy spectrum, noted for its high energy yield and clean combustion. Nonetheless, the production, storage, and utilization of hydrogen, as investigated by Nicolay et al. [8], encounter significant technical and economic hurdles. The challenges include the need for efficient and cost-effective production methods, safe and compact storage solutions, and the development of infrastructure to support widespread use.

Hydrogen, in particular, stands out due to its significant potential in reducing greenhouse gas emissions, although it produces up to 2.5 times more water vapor than conventional kerosene propulsion systems. According to Owen et al. [1], the strategic adoption of hydrogen and other alternative fuels could lead to a substantial decrease in CO_2 emissions, ranging from 2 to 12% by 2050. Insights into the development and challenges of integrating LH_2 fuel cell technology within aircraft propulsion systems have seen significant breakthroughs. Commercial applications of low-temperature proton-exchange membrane fuel cells (LT-PEMFCs), as demonstrated by the aerospace company Hypoint, sourced by [9], have already achieved 2 kW/kg power density. Practical applications see a reduction to 0.75–1 kW/kg at the system level due to the added weight of auxiliary components [9]. This context brings into focus the work by Abu Kasim et al. [10]: a comprehensive design and analysis of a turbocharged Proton-Exchange Membrane Fuel Cell Power System (PEM-FCPS) for retrofitting the Cessna 208 Caravan aircraft. Powered by LH_2, the proposed system incorporates four Ballard PEMFC stacks, each generating 140 kW, and is supported by two Garrett G25-550 turbochargers to ensure performance consistency across varying altitudes, achieving 43% efficiency and 28 kg/h hydrogen consumption over a 1.5 h flight (350 km). Designed for emissions-free electricity, the system demonstrated reliability with a failure rate below 1.6 per million hours, comparable to commercial jet engines. This analysis showcases the high potential of PEMFC in small and short-range aircraft but emphasizes its limitations in high-range aircraft, which need further investigation. The study also notably lacks a comprehensive emissions analysis and an assessment of the economic implications of such conversions. These gaps underscore the necessity for further research to fully understand the broader applicability, environmental benefits, and cost-effectiveness of fuel cell technology in aviation.

Alternative fuel feasibility studies align with the objectives of industry demonstrators and manufacturers. Findings from Hypoint, sourced from Massaro et al. [5], indicate that by 2025, a regional aircraft capable of carrying 75 passengers over 800 nautical miles could be viable using fuel cell technology at 3 kW/kg for PEMFC. This would entail a 2.21% increase in energy requirements and a 26% increase in the maximum takeoff weight (MTOW) relative to traditional aircraft, showcasing the growth hydrogen fuel cells for aviation are exhibiting. However, PEMFCs have shown efficiencies of greater than 50%, although limited in comparison to efficiencies that solid oxide fuel cell (SOFC) hybrids can achieve by recycling their high temperatures. The investigation highlighted by Rupiper et al. [11] into flame-assisted SOFCs, which are incorporated between two combustion stages in a gas turbine, revealed a configuration that eliminates the need for external heating or heat exchangers for the SOFC, thus reducing startup times and yielding a 24.5% increase in system efficiency over conventional gas turbine systems. Further, Seitz et al. [12] explored a parallel hybrid architecture where the SOFC system operates independently of the gas turbine cycle. This setup, while powering separate propulsors or aircraft subsystems, also leverages the water vapors produced by the SOFC to enhance the efficiency of the gas turbine core, achieving up to a 62% reduction in NO_x emissions and a 7.1% improvement in block fuel burn compared to baseline engines. Moreover, Liu et al. [13] and Collins and Mclarty [14] delved into the potential of turbo-electric hybrid systems combining SOFCs, batteries, and turbine generators, demonstrating potential system efficiencies of up to 65–75%. These observations emphasize the significant potential of SOFC technology in surpassing PEMFC by enhancing efficiency and minimizing the environmental footprint of aviation propulsion systems. A primary challenge in hybrid propulsion systems lies in the complex integration of different energy conversion methods and propulsion architectures, necessitating coordinated and compact thermal management strategies. Additionally, SOFCs face operational challenges due to their high-temperature requirements and material brittleness, as well as design limitations that often restrict them to planar configurations,

which may not be optimal for all aircraft designs. The integration of SOFCs into aircraft systems is considerably less explored and commercialized compared to PEMFCs. This paper aims to explore the potential and implications of incorporating SOFC technology into aviation.

Hydrogen (H_2) combustion and fuel-cell-powered electric propulsion have emerged as leading alternatives for reducing pollutants, with their potential extensively studied in recent literature [15]. The inherent characteristics of hydrogen, including its broad availability and high volumetric energy density, position it as a viable solution for carbon mitigation. Notably, H_2 combustion primarily produces NO_x and H_2O, significantly reducing greenhouse gas emissions. This technology encompasses hydrogen-powered turbofans, turboprops, or propellers, which convert chemical energy into mechanical energy through combustion. Additionally, the electric powertrain, powered by a hydrogen SOFC hybrid system, offers an alternative by providing the necessary energy to operate electric propulsors such as electrified turbofans and turboprops. The adoption of fuel cells in aviation is advantageous due to their rapid refueling capabilities and enhanced efficiency when utilized in conjunction with hydrogen fuel [16].

Several leading engine manufacturers, including Rolls Royce, along with numerous startups, have initiated plans to showcase fuel cell technologies and hydrogen combustion applications [15]. However, both H_2 combustion engines and SOFC hybrid systems necessitate substantial tank capacities for storing cryocompressed or LH_2 onboard, alongside more complex powertrains. Rivard et al. highlight that LH_2 possesses a density of 71 kg/m^3 at 1 bar, although still lower than conventional fuels. Moreover, advancements in storage technology have enabled cryocompressed hydrogen to achieve densities up to 81 kg/m^3, presenting an even more efficient storage option [17]. Despite these advancements, the cryogenic nature of LH_2 complicates handling and necessitates careful selection of storage vessels, such as vacuum insulated or Dewar flasks. Managing the challenges associated with LH_2 includes addressing boil-off to align with fuel consumption and developing effective thermal insulation strategies to mitigate weight concerns [17]. Prewitz et al. further elucidate the implications of LH_2's large storage requirements and the associated power systems, which could potentially affect the aircraft's range and balance [18]. As such, a structured methodology is imperative for evaluating the tradeoffs involved in adopting these alternative fuels and power sources in contemporary aircraft designs. In the realm of passenger aircraft, research has predominantly concentrated on the design and modeling of hydrogen-powered propulsion systems [15]. Despite this focus, a comprehensive comparison of alternative fuel types within aircraft propulsion systems remains scant, especially in terms of assessing the feasibility of substituting kerosene with fuel cells and hydrogen. This gap underscores a significant need for further research, as existing studies have mainly addressed performance and range, often overlooking factors related to usability and operational sustainability. Consequently, this study advocates for an approach centered on retrofitting existing aircraft with alternative fuel systems, as opposed to designing new aircraft from scratch. Such a perspective aims to furnish a reliable evaluation of the potential advantages offered by alternative fuels in modern aviation.

Building upon the discussion of hydrogen's potential and the complexities of its integration into aviation, this study delineates a comparative analysis framework. This framework evaluates conventional kerosene-powered aircraft against aircraft retrofitted with H_2 combustion systems and SOFC-powered alternatives. The retrofitting process involves the design of LH_2 tanks and an SOFC powertrain tailored to the operational and feasibility requirements of existing kerosene-powered aircraft. Given the nontrivial nature of integrating hydrogen technologies, owing largely to the need for larger tanks and powertrain modifications, this framework employs a lifecycle emissions assessment alongside a mission implementation cost analysis. These tools facilitate a nuanced comparison of the environmental and economic tradeoffs associated with the adoption of hydrogen, fuel cell-hydrogen hybrids, and conventional power sources. A case study focusing on a Cessna Citation 560XLS+ business jet serves to illustrate the practical implications for emissions reduction, contrail mitigation, and the assessment of performance and feasibility tradeoffs. Notably, business jets, which contribute 0.04% to annual carbon emissions, emerge as prime candidates for early adoption of zero-emission technologies. This is underscored by findings that hydrogen-powered business jets could achieve up to a 34% net reduction in energy consumption [19,20], highlighting the significant efficiency gains and emission reduction potential that underpin the methodology explored in the subsequent sections.

II. Methodology to Assess Emissions and Performance Tradeoffs for a Retrofitted-Solid-Oxide-Fuel-Cell- and Hydrogen-Powered Aircraft

The methodology to model the alternative fuel emissions for a proposed aircraft vehicle is presented in Fig. 1. The inputs to the modeling framework include the aircraft characteristics, such as empty and takeoff weights, overall efficiency, and lift-to-drag ratio. In addition, the alternative fuel type is defined by the heat energy available per unit weight of fuel and mission characteristics such as range and cruising altitude. These parameters define the aircraft's cruising performance in the flight profile module. Within the flight profile module, the weight of the fuel necessary to complete the mission is determined and inputted into the H_2 tank configuration module and the emissions module. The tank configuration module

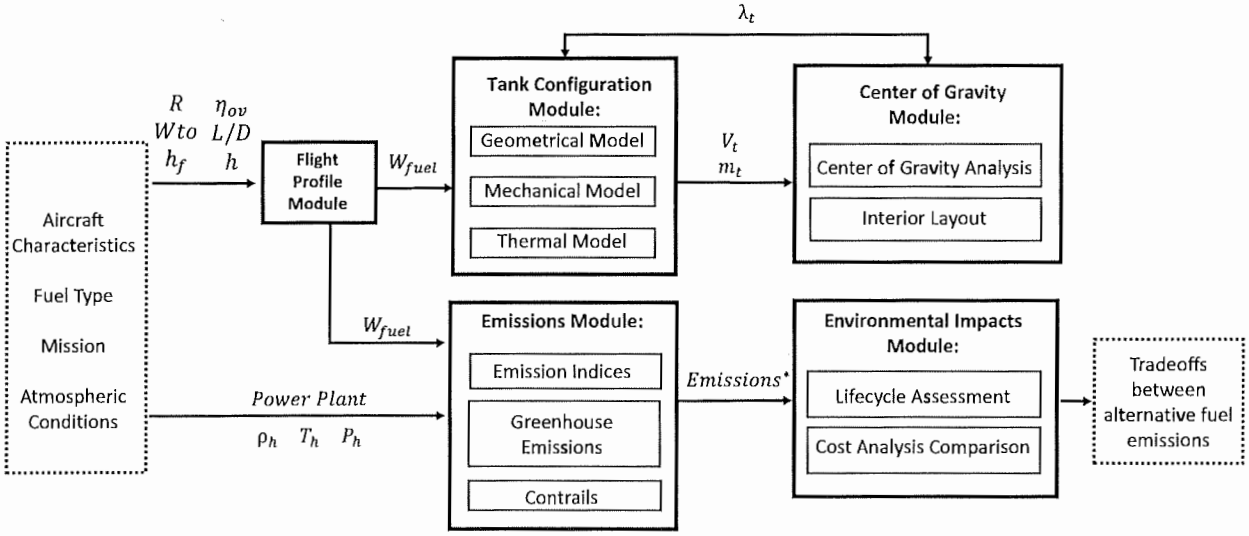

Fig. 1 Modeling framework of the methodology to assess emissions and performance tradeoffs for a retrofitted SOFC hybrid and H_2-powered aircraft.

models the shape, insulation, and volume of an H_2 cylindrical tank that meets the power requirements defined by the weight of the fuel. The tank volume and mass are then outputted into the center of gravity (CG) module. This module determines the CG change within the flight envelope of the aircraft by simultaneously placing the tanks in the interior layout. A tank sizing constraint is fed back into the tank configuration module if such CG requirements are not feasible for the same number of passengers. The tank configuration module updates the tank design, and the weight of the fuel is remodeled to account for the weight of passenger removal. If such changes occur, either a refueling stop is required or a second flight of the same mission will keep the number of passengers constant for the same range. Such consequences are accounted for in the lifecycle emissions and cost modeling covered in detail in the following section.

Furthermore, the weight of the fuel, the mission atmospheric conditions, and the power plant for each alternative fuel type are inputted into the emissions module. Within this module, the emissions per segment are analyzed by their emission indexes, greenhouse gas emissions, and contrails. Such segment emissions are then inputted into the environmental impact module. This module implements the mentioned lifecycle assessment and cost analysis to output the tradeoffs between alternative fuel power plants per mission. The details of this framework are further discussed in the following sections.

A. Flight Profile Module

The methodology presented in the previous section consists of a baseline range mission profile to compare the alternative fuel sources with a baseline kerosene gas turbine combustion flight procedure. A constant range approach analysis is implemented in order to design an alternative fuel tank and power train that satisfies insulation, CG, and power constraints. The Breguet range equation determines the weight of the fuel required to fly the given mission for the baseline and alternative fuel sources [21].

Hydrogen combustion would require some changes to the design of the engines due to the different properties of hydrogen, such as a higher adiabatic temperature and faster flame speeds. Such changes include a smaller combustion chamber, the addition or modification of a pump, supply pipes, control valves, heat exchanger, and turbine system, as depicted in Fig. 2, which outlines a hydrogen-fueled multistage gas turbine layout. The aforementioned hydrogen combustion system replaces the conventional turbofan for the H_2-combustion-powered aircraft studied in this paper, portrayed in Fig. 3. In addition, a heat exchanger must also be added to heat the cryogenic hydrogen liquid fuel before combustion [22]. Stefan et al.'s review highlights key challenges for hydrogen combustion in aviation, particularly the need for materials that withstand high temperatures and hydrogen-indueed corrosion, as found in hydrogen-fired gas turbines. Stefan et al. emphasize the importance of developing advanced coatings and alloys, especially considering the larger temperature gradients and increased steam content in hydrogen combustion, which pose risks to component durability and efficiency. The study also notes the necessity for further research into hydrogen embrittlement, particularly for parts made via additive manufacturing [23]. These material challenges form a crucial part of the overall technological hurdles to integrating hydrogen combustion systems into aviation.

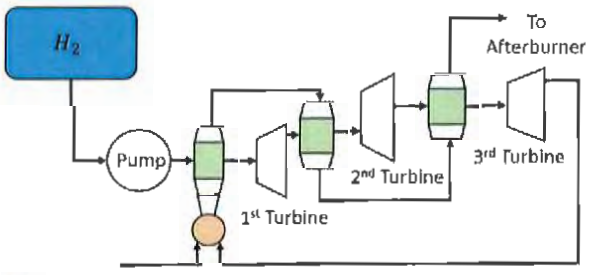

Fig. 2 Hydrogen-fueled multistage gas turbine configuration.

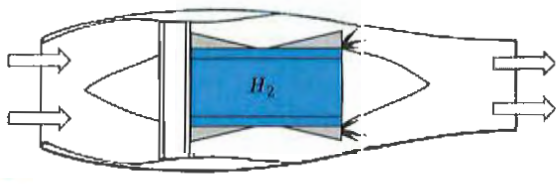

Fig. 3 Hydrogen combustion gas turbine.

Cryogenic hydrogen tanks become very heavy depending on the design parameters, stored pressure, temperature, and acceptable boil-off rates. Fortunately, for aircraft applications, less insulation is required for short periods of flight at a relatively high boil-off rate. The design choices of a number of tanks and storage locations affect the final mass and volume of the hydrogen storage system. The high gravimetric energy density of hydrogen of 120 MJ/kg is favorable since mass reduction is critical during flight. Hydrogen needs to be stored at its critical temperature and pressure of 33.15 K and 1300 kPa. However, the main challenge in aviation lies in the mass and volume that such cryogenic tanks occupy. Hydrogen density varies between a low of 0.08375 kg/m^3 in gaseous form and a high of 81 kg/m^3 in cryocompressed liquid form [24]. Such densities are low when compared to the densities of kerosene, which vary from a low of 775 kg/m^3 to a high of 840 kg/m^3.

Another alternative, the SOFC hybrid power plant configuration, is evaluated for a constant-range mission. Such an SOFC hybrid includes a battery and liquid H_2 tanks to provide electrical power with zero emissions. Proton exchange membrane fuel cells (PEMFC) and SOFC advantages include independent power and energy scaling at efficiencies up to 60%. Unfortunately, fuel cells lose efficiency with altitude due to lower atmospheric pressure. Hence, for aircraft applications, a hybrid SOFC gas-turbine system can convert fuel cell waste heat to electric power and pressurize a fuel cell. The overall power system efficiency has been shown to provide slightly higher efficiencies in the range of 10–20%, approximately for a conventional aircraft. Wilson et al. [25] present a thermodynamic model aimed at evaluating the feasibility and performance of a high-performance SOFC/GT hybrid power system tailored for electric aviation. Their findings highlight the potential of such systems to achieve fuel-to-electricity conversion efficiencies significantly higher than those of conventional gas turbine engines, thereby underscoring the importance of these hybrid systems in the pursuit of net zero emissions for the aviation sector. Challenges remain, particularly in balancing plant design and integrating dynamic simulation capabilities, to fully realize the potential of these technologies. The validation of their model against NASA's SOFC model and its application in constructing a 1 MW SOFC/GT hybrid power system for aircraft propulsion demonstrate the feasibility of achieving efficiencies greater than 75% under standard cruise conditions, pointing toward the necessity of further research and development to address the identified challenges and enhance system reliability and lifespan [25].

In the retrofit model assumptions for the SOFC hybrid system, which includes components such as a gas turbine, heat exchangers, a compressor, a generator, a battery, and an LH_2 tank, power assumptions for the fuel cell, battery, and motor-specific densities are based on state-of-the-art (SOA) technology expected to be commercially available. Specifically, the SOFC exhibits gravimetric and volumetric power densities of 2.5 kW/kg and 7.5 kW/L, respectively [26]. These figures suggest that the SOFC hybrid, as designed, offers up to five and seven times higher gravimetric and volumetric power densities than those found in commercially available designs to date. Advanced research indicates even higher specific densities for fuel cells and motors, with findings pointing to 4.0 kW/kg for fuel cells and 10 kW/kg for motors [16]. The SOFCs exit temperature is noted to be 944°C, showcasing the potential of recycling heat within the system [25]. The battery technology utilized within this hybrid system features a volumetric energy density of 0.67 kW·h/L and a

gravimetric energy density of 0.35 kW·h/kg [14]. Moreover, the gas turbine, integral to the SOFC hybrid configuration, is characterized by a volumetric density of 8000 kg/m^3 and a gravimetric power density of 4.4 kW/kg, illustrating the compact and efficient design achievable in modern gas turbines [27]. The cycle efficiency of the SOFC/GT system is conservatively assumed to be 70%, still indicating an improvement over conventional systems [14]. Lastly, the inclusion of a cryocooler with a mass specific power of 3 kg/kW further demonstrates the comprehensive approach taken to address thermal management challenges within the system [28]. The gas turbine's power output is chosen as 538 kW to be aligned with the SOFC's capacity to ensure optimal integration and performance efficiency within the hybrid system [27]. This assumption set shown in Table 1 forms the basis for the SOFC hybrid power train.

The SOFC hybrid power train system consists of multiple components, such as an electric motor, the SOFC, a generator, a pump, a cryogenic tank, and other components seen in Fig. 4. The cryogenic tank stores LH_2 fuel that vaporizes once vented from the tank. The hydrogen is then heated in a heat exchanger (HX) that acts as a fuel heater. The HX recycles heat exiting the turbine, and a fuel pump increases the pressure of the hydrogen before it is fed into the anode of the fuel cell. Oxidation reactions occur within the anode, and compressed air from the compressor is then heated in the combined HX. Such air then inlets into the cathode, where the reduction reactions occur. Compressed air flow helps maintain and increase fuel cell performance at flight altitude. The turbine is utilized to power the compressor and generator, while the generator produces electricity that can be stored in the battery or used for propulsion in the electric motor.

Table 1 Power train for SOFC hybrid

Parameter	Value
SOFC volumetric density, kW/kg	2.5 [26]
SOFC gravimetric density, kW/L	7.5 [26]
SOFC exit temperature, °C	944 [25]
Motor density, kW/kg	7.06 [16]
Battery volumetric density, (kW · h)/L	0.67 [14]
Battery gravimetric density, (kW · h)/kg	0.35 [14]
SOFC/GT cycle efficiency, %	70 [14]
GT volumetric density, kg/m^3	8000 [27]
GT gravimetric density, kW/kg	4.4 [27]
Cryocooler mass specific power, kg/kW	3 [28]
Gas turbine power, kW	538 [27]

The aforementioned H_2 combustion and SOFC hybrid system are utilized to power the constant range from the baseline kerosene flight procedure. The Breguet range equation for heat energy available per unit weight accounts for such changes within this module and results in the fuel weight outputted into the tank module. A sample implementation of this methodology for both H_2 combustion and SOFC hybrid system is performed on a business jet in Sec. III.

B. Tank Configuration Module

Given the design fuel weight from the previous module, tanks are modeled for a retrofitted aircraft in the tank configuration module. The design of such tanks follows the approach in Fig. 5. The tank module evaluates geometrical, material, and thermal models that serve as feasible variables within the design space [29]. Such tank modeling is governed by Eqs. (1–9).

1. Geometrical Model

The geometrical model rigorously defines the tank geometry and the necessary volume of storage to satisfy power constraints. The tank is architecturally shaped as a cylinder with hemispherical ends —a design celebrated for its superior pressure distribution, making it a prevalent choice for pressurized vessels [16]. To buffer pressure variations due to hydrogen boil-off, an excess volume V_i, set at 7.2%, is accounted for in the calculations. The storage volume, V_t, is meticulously calculated to ensure that the tank can accommodate the required mass of hydrogen, M_{H_2}, while compensating for boil-off through an additional volume, V_i, and considering the density of LH_2, ρ_{LH_2} as shown in Eq. (1). The choice of a cylindrical tank with hemispherical ends optimizes the pressure distribution within the tank, minimizing stress concentrations and enhancing structural integrity, as the volume of this specific geometrical configuration is represented in Eq. (2). Further, the mass of the filled capsule is determined by Eq. (3) to assess the impact of the stored hydrogen on the overall aircraft structure, a crucial factor affecting aircraft performance and fuel efficiency. The tank's design also incorporates meticulous calculations for the wall thickness. Equation (4) determines the wall thickness of the cylindrical section, considering the design pressure P_{des}, the material's tensile strength σ_a, and the efficiency of the welding process, e_{weld}. This ensures that the tank wall can withstand internal pressure without compromising safety or integrity. Moreover, the hemispherical ends of the tank, which are subject to unique stress distributions, require a specialized approach for determining their thickness, as captured by Eq. (5). This formula takes into account the design pressure, the stress factor K, the material

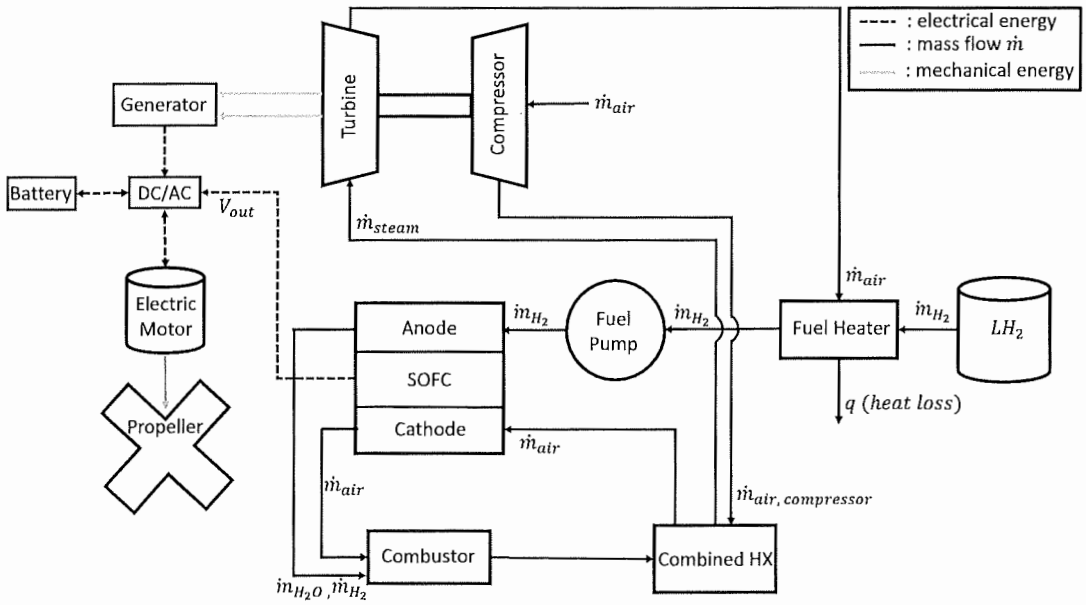

Fig. 4 Power train SOFC hybrid for medinm-range and long-range aircraft designed for fuel cell hybrid.

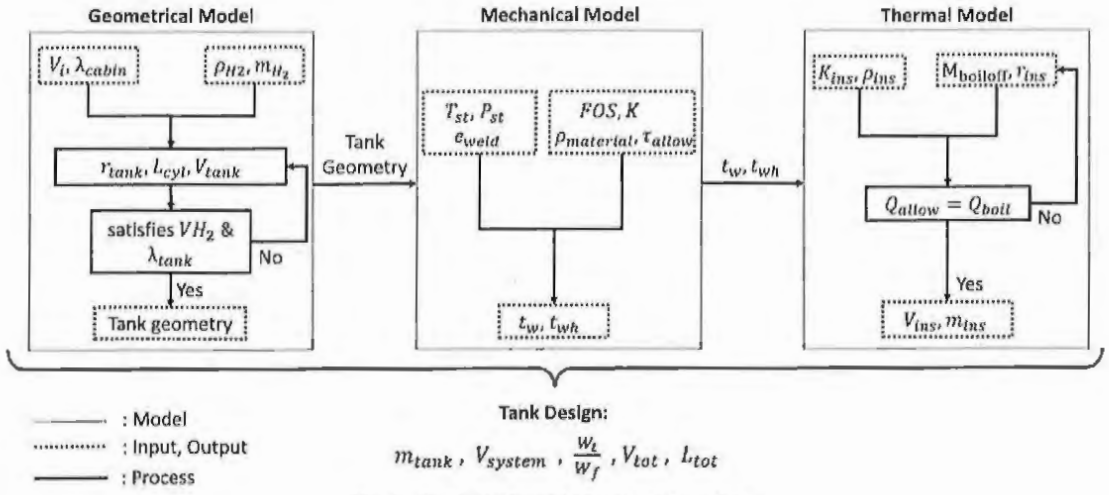

Fig. 5 Tank configuration module flowchart.

properties, and the welding quality, reinforcing the tank's structural integrity comprehensively. In essence, these equations are meticulously chosen to ensure a holistic and accurate representation of the tank's geometrical, physical, and mechanical properties. They collectively safeguard the tank's structural integrity, aligning with mechanical, safety, and performance specifications, ultimately delivering a reliable and effective hydrogen storage solution.

$$V_t = \frac{M_{H_2}(1 + V_i)}{\rho_{LH_2}} \tag{1}$$

$$V_t = \frac{4\pi r^3}{3} + r^2 \pi L \tag{2}$$

$$m_{\text{filledcapsule}} = \rho \pi r_1^2 \left(L_1 - \frac{2}{3} r_1 \right) \tag{3}$$

$$t_w = \frac{P_{\text{des}} d_o}{2\tau_{\text{allow}} e_{\text{weld}} + (0.8 P_{\text{des}})} \tag{4}$$

$$t_{\text{wh}} = \frac{P_{\text{des}} d_o K}{2\tau_{\text{allow}} e_{\text{weld}} + 2P_{\text{des}}(K - 0.1)} \tag{5}$$

$$K = \frac{1}{6}\left(2 + \frac{d}{d_1}\right) \tag{6}$$

2. *Mechanical Model*

In the mechanical model, the derived geometry and selected materials precisely determine the tank wall thickness. Aluminum (4.4% Cu) 2014-T6 is chosen for its optimal strength-to-weight ratio and fatigue resistance, which are crucial for aerospace applications. This material, coupled with evacuated aluminum foil and fluffy glass mats for insulation, as recommended by Rivard et al. [17], creates a robust yet lightweight barrier, effectively reducing thermal conductivity. The factor of safety (FOS) is judiciously set at 1.3, aligning with standard engineering practices to balance durability and material efficiency. This ensures the tanks are resilient yet not overdesigned, maintaining a weight that is typically 15–30% of the LH_2 weight, potentially less than 15% with reduced hydrogen vaporization rates as noted by Baroutaji et al. [16]. Such optimization is crucial for aircraft performance and fuel efficiency. The model integrates the inner vessel within a vacuum, defined by precise geometrical thickness, to minimize heat transfer and enhance the thermal stability of LH_2. These dimensions, along with the selected materials, are integrated into the thermal module to determine the optimal insulation thickness, ensuring the system meets stringent thermal requirements while optimizing for weight and structural integrity, reflecting sophisticated aerospace engineering.

3. *Thermal Model*

The thermal model is developed to determine the optimal wall insulation thickness by considering the material properties, an acceptable boil-off rate, and the corresponding acceptable rate of heat transfer. The design criteria are based on Eqs. (7–10), which are instrumental in modeling the heat transfer dynamics within the insulation layer. The insulation thickness is specifically tailored to maintain a boil-off rate of 0.1% per hour, as suggested by Baroutaji et al. [16]. This particular rate is chosen because it strikes a balance between insulation performance and the minimization of insulation material, which in turn reduces both the cost and mass of the system. The design allows for 20% of the stored hydrogen to be vented per hour, optimizing the system for a 288.15 K outer surface temperature to maximize the range and flight time of the aircraft. The inner vessel, situated within a vacuum, is designed with precise geometrical thickness and insulation parameters to meet the tank sizing constraint λ_{tank}, as illustrated in Fig. 6. This constraint is crucial as it feeds into the CG module, influencing the overall aircraft design. The equations forming the core of the thermal model are instrumental in elucidating and forecasting the system's behavior under a spectrum of conditions. The Nusselt number (Nu) in Eq. (7), as derived from Colozza and Kohout [30], serves as a fundamental component in hydrogen tank thermal modeling, signifying the ratio of convective to conductive heat transfer across the boundary layer. Tailored for cylindrical tank geometries, this specific correlation incorporates the flow characteristics of hydrogen, captured by the Reynolds number (Re_D), and the fluid's intrinsic properties, as indicated by the Prandtl number (Pr). This correlation is instrumental in determining the convective heat transfer coefficient, a key factor in accurately modeling the temperature distribution and managing heat flow in and out of the hydrogen storage tank. Equation (8), which delineates the rate of heat transfer (Q), is foundational for deducing the energy requisite for the phase transition of hydrogen, taking into account the mass flow rate ($\dot{m}$) and

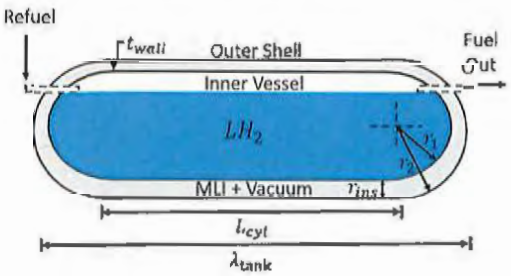

Fig. 6 H_2 cryogenic tank geometry definition.

the latent heat of vaporization (h_{fg}). The set of equations introduces a more comprehensive approach to heat transfer analysis, taking into account conduction (Q_{cond}), convection (Q_{conv}), and radiation (Q_{rad}) heat transfers, represented in the total heat transfer equation (Q_{total}). These equations collectively form a robust framework for designing an efficient and effective thermal management system for hydrogen storage in aircraft applications. These equations are critical for ensuring the thermal management system is designed with precision, taking into account the necessary physical phenomena to maintain the hydrogen in its desired state, and ensuring the safety, efficiency, and effectiveness of the aircraft's power system.

$$Nu_D = \left[0.60 + 0.287 \frac{Re_D^{1/6}}{\left[1 + \left(\frac{0.559}{Pr}\right)^{9/16}\right]^{8/27}} \right]^2 \tag{7}$$

$$Q = \dot{m} \times h_{fg} \tag{8}$$

$$Q_{\text{total}} = Q_{\text{cond}} + Q_{\text{conv}} + Q_{\text{rad}} \tag{9}$$

$$\begin{aligned} Q_{\text{total}} = {} & \frac{2\pi L k (T_o - T_i)}{\ln(r_2 r_1)} + \frac{4\pi r_1 r_2 k (T_o - T_i)}{r_2 - r_1} \\ & + h_{conv}(2\pi r_2 L + 4\pi r_2^2)(T_o - T_{\text{atm}}) \\ & + \varepsilon\sigma(2\pi r_2 L + 4\pi r_2^2)(T_o^4 - T_{\text{atm}}^4) \end{aligned} \tag{10}$$

C. Center of Gravity Module

1. *Center of Gravity*

A weight and balance analysis evaluates the feasibility of the tank design outputted from the tank configuration module. The change in CG location from the operational limits of the retrofitted conventional kerosene-powered aircraft is modeled from an already existing FAA-approved operational envelope found in [31]. The net change in CG is modeled to determine if the new retrofitted CG is within the minimum and maximum limits of the aforementioned envelope. Assuming the CG lies at 25% mean aerodynamic chord (MAC) in the existing weight and balance diagram, the change in CG is determined by the shifted weight and potential moment arm [32]. Such moment arm is simultaneously obtained in the interior layout of the aircraft within this module. The weight per passenger is estimated to be 93 kg for domestic flights [33]. The weight of a fully stocked refreshment center is assumed to be 147 kg, with two full carts, while the weight of the lavatory is estimated to be 60 kg. The change in weight from each alternative retrofitted fuel configuration is obtained by summing all changes in moments from either removing a seat or adding a tank, among others.

2. *Interior Layout*

Simultaneously within the CG module, a potential change in the moment arm is obtained from an interior layout map of the existing aircraft. A sample case interior layout for a business jet is used in Sec. III to obtain the dimensions of the interior, the baggage compartment, and the overall aircraft specifications for a Cessna Citation 560XLS+. Such dimensions are used to evaluate and constrain the size of the tanks by placing them in a position that results in a feasible CG within the aforementioned envelope limits and FAA aisle width and seat pitch regulations. After a feasible tank sizing constraint is reached in the tank configuration module, the final weight of the fuel is inputted into the emissions module. Such weight of the fuel will account for passenger weight removal in case passenger seats need to be removed to make room for tanks.

D. Emissions Module

The emissions analysis provides a comparative study of traditional kerosene and advanced H_2 combustion and SOFC hybrid propulsion systems. The study models complete kerosene combustion to yield CO_2 and H_2O, while incomplete combustion produces CO, NO_x, SO_x, and HC. In contrast, complete H_2 combustion is expected to emit only H_2O, with NO_x as the primary byproduct during incomplete combustion, without the emissions of CO, HC, or SO_x. The analysis assumes minimal unburnt H_2 emissions due to the employment of advanced H_2 management and combustion technologies, including lean, fully premixed (LFP) combustors, which are designed to ensure thorough mixing and complete combustion of hydrogen fuel. This assumption is supported by the work of Palies [34], who indicates that LFP combustors are effective in reducing unburnt fuel, aligning with the goal of zero-unburnt fuel in hydrogen-powered aviation. This premise is supported by computational simulations that demonstrate the efficacy of LFP combustors in reducing unburnt fuel, aligning with the zero-unburnt fuel efficiency posited for LFP configurations in hydrogen combustion scenarios [34]. While the ideal scenario presents negligible H_2 emissions, practical implementations will require strategies for capturing or neutralizing any unburnt H_2 to fully leverage the environmental benefits and maintain safety standards [35]. The SOFC hybrid system, which also utilizes H_2 as a fuel, is mainly associated with the emissions of H_2O and NO_x. The detailed emission profiles of these advanced propulsion systems will be further discussed in the following sections, offering insights into their potential environmental impacts.

The emissions analysis provides a comparative study of traditional kerosene and advanced H_2 combustion, as well as SOFC hybrid propulsion systems. This study models the complete combustion of kerosene to yield CO_2 and H_2O, while incomplete combustion produces CO, NO_x, SO_x, and HC. In contrast, complete H_2 combustion is expected to emit only H_2O, with NO_x being the primary byproduct during incomplete combustion, without the emissions of CO, HC, or SO_x. The analysis assumes minimal unburnt H_2 emissions due to the employment of advanced H_2 management and combustion technologies, including LFP combustors. These combustors are designed to ensure thorough mixing and complete combustion of hydrogen fuel. This assumption is supported by the work of Palies [34], indicating that LFP combustors are effective in reducing unburnt fuel, thereby aligning with the goal of achieving zero-unburnt fuel in hydrogen-powered aviation. Furthermore, computational simulations have demonstrated the efficacy of LFP combustors in reducing unburnt fuel, aligning with the zero-unburnt fuel efficiency posited for LFP configurations in hydrogen combustion scenarios [34]. While the ideal scenario presents negligible H_2 emissions, practical implementations will necessitate strategies for capturing or neutralizing any unburnt H_2 to fully leverage the environmental benefits and maintain safety standards [35]. The SOFC hybrid system, which also utilizes H_2 as fuel, is primarily associated with the emissions of H_2O and NO_x. The detailed emission profiles of these advanced propulsion systems will be further discussed in subsequent sections, offering insights into their potential environmental impacts.

1. *Emission Indices*

The International Civil Aviation Organization (ICAO) Engine Emissions Databank (EED) is employed to acquire the Emission Indices (EI) for noncruise phases of flight for kerosene-powered aircraft. The EI for incomplete combustion of HC and CO during cruise is averaged at 0.4 and 0.6 g/kg, respectively, as reported by Wayson et al. [36]. Emissions of SO_x are omitted in this analysis due to the absence of corresponding data in the ICAO databank. The investigation concentrates on the principal emissions shared across the three technologies under review. Typically, the EI for NO_x ranges from 12 to 16 g/kg [36], influenced by the engine design's flame temperature. For simplicity, a median value of 14 g/kg is adopted for cruise conditions. This assumption is considered safe and pragmatic for comparative purposes, especially when specific combustion conditions (lean vs rich) or the application of emission mitigation technologies are not explicitly detailed. It is acknowledged that NO_x emissions from hydrogen combustion can vary significantly depending on the technology used for emission mitigation. For instance, Therkelsen et al. [37] have shown that hydrogen combustion can lead to higher NO_x emissions due to the higher flame temperatures associated with hydrogen, despite efforts to achieve near-uniform fuel/air mixing. This underscores the inherent challenges in managing NO_x emissions from hydrogen-fueled

engines, where even advanced mixing technologies cannot fully mitigate the thermal NO_x formation inherent to hydrogen's combustion properties. Conversely, advancements in emission reduction technologies have shown significant potential in lowering NO_x emissions from hydrogen-fueled aircraft, with reductions up to 90% compared to kerosene combustion, achieved through the implementation of technologies such as water injection [18,38]. This illustrates the effectiveness of such technologies in overcoming the thermal NO_x challenges associated with hydrogen combustion. Furthermore, the rich-quick-lean (RQL) combustion strategy proposed by Ingenito et al. [39] provides an effective framework for reducing NO_x emissions in high-speed hydrogen-fueled vehicles to ICAO acceptable values. By optimizing the equivalence ratio in the rich combustion stage and taking advantage of the wider flammability limits of the hydrogen flames in the lean combustion stage dramatic reduction in NO_x emissions were demonstrated, further supporting the argument for technological variability in hydrogen combustion outcomes [39]. Given the vast variability in hydrogen combustion NO_x emissions influenced by technology and operational conditions, adopting a median EI_{NO_x} value of 14 g/kg for comparative purposes across all technologies is analyzed, including the SOFC hybrid system. In this context, NO_x emissions are primarily generated not by the fuel cell itself but by a hydrogen combustor/micro-gas-turbine system operating at potentially higher temperatures. This standardized assumption facilitates a consistent comparison while acknowledging the diverse technological landscape and the potential for significant emission reductions with the right combination of fuel, technology, and operational strategies. Furthermore, in the case of kerosene combustion, the fuel composition significantly influences H_2O and CO_2 emissions, with a higher H/C ratio yielding more water and less CO_2. The EI for CO_2 is calculated by considering the carbon content in the fuel, the molar mass of CO_2, and the molar mass of carbon, resulting in 3.15 kg/kg. Similarly, the EI for H_2O, derived through the same methodology, is found to be 1.25 kg/kg. This approach ensures a consistent and comparative framework for assessing the environmental impact of both hydrogen and kerosene-fueled aircraft across different flight conditions.

2. Emissions

The CO_2 and H_2O emissions of kerosene are compared to the retrofitted H_2 combustion and SOFC-hybrid-system-powered aircraft. Such an emissions model assumes a constant percent thrust per segment and a constant aircraft thrust-specific fuel consumption (TSFC). Each segment emission is modeled by dividing the flight profile into the segments seen in Table 2. The flight profile is designed to optimize aircraft ground operations to reduce emissions and local air quality impacts [40,41]. The thrust per engine is taken at 100% for takeoff, 85% for climb, 30% for approach, and 7% for descent and idle, which matches the suggestions of the ICAO standard landing and takeoff cycle regulations [42]. The time to climb and descend is assumed to be 30 minutes. Although taxi/idle time varies by airport, an average value of 23 minutes is assumed for this analysis. This choice is justified by aiming to represent a typical ground operation time that balances between shorter durations at less congested airports and longer periods at major hubs. Thereby providing a realistic and rather conservative average for a broad spectrum of flight operations. For the cruise portion of the flight, Eq. (11) models the mass fuel burned to obtain the complete emissions of CO_2, H_2O, CO, HC, and NO_x. A sample of implementing this methodology for modeling emissions is demonstrated in detail in Sec. III.A.

Table 2 Assumed flight profile segments

Segment	Duration, min	Thrust, %
Takeoff	0.7	100
Climb	30	85
Descent	30	7
Approach	4	30
Taxi/idle	23	7

$$E_x = m \times \mathrm{EI}(X) \tag{11}$$

3. Contrails

The likelihood of contrail formation using kerosene, H_2 combustion fuel, and an SOFC hybrid-powered aircraft is modeled using mass and energy balances to determine the mixing line slope G. An aircraft exhaust plume mixes isobarically with exhaust air and can lead to the possibility of contrail formation [43]. Contrails may form by the mixing of hot and humid air with cold ambient air below a critical temperature threshold, as defined by the Schmidt–Appleman criterion [43], which is modeled by Eq. (12):

$$G = \frac{P_a \mathrm{EI}(H_2O) C_{p,\mathrm{Air}}}{\epsilon_{H_2O} \mathrm{LHV}_{\mathrm{fuel}} (1 - \eta_{\mathrm{overall}})} \tag{12}$$

Such contrails are evaluated since they can increase the overall warming effect due to trapped heat in the atmosphere and affect cooling from reflected sunlight [44]. The overall efficiency of the aircraft is assumed to be constant for all three configurations. The H_2 combustion and SOFC hybrid are expected to have a shallower slope than kerosene due to a higher $\mathrm{LHV}_{\mathrm{fuel}}$ value of 120 MJ/kg. Such a value is higher when compared to the conventional lower 43 MJ/kg kerosene $\mathrm{LHV}_{\mathrm{fuel}}$, as shown in Sec. III.A. However, an increase in the mixing slope G arises from the higher EI of H_2O when using LH_2 fuel. The persistence of contrails is not explored due to the location dependence of atmospheric conditions at every point of the duration of a single flight.

E. Environmental Impacts Module

1. Lifecycle Assessment

A complete lifecycle analysis (LCA) of CO_2 evaluates the environmental effects of a conventional kerosene-powered aircraft, a retrofit H_2 combustion aircraft, and a retrofit SOFC-hybrid-powered aircraft. The lifecycle emissions are modeled for the various stages of fuel extraction, transport, processing, and storage sectors known as well-to-tank (WTT), and a combustion sector known as tank-to-wheel (TTW), as shown in Fig. 7. Such LCA evaluates the consequences of eliminating the dependency of aviation upon dwindling crude oil resources, as well as the overall contribution of aviation to the anthropogenic greenhouse effect [45]. The carbon intensity of kerosene fuel can vary depending on the region, the refinery, and the crude oil well. Various studies have estimated that the carbon intensity of jet fuel ranges from 85 to 95 g of CO_2/MJ [46]. The combustion of fuel contributes to a portion of 73 g of $CO_{2\,eq}$/MJ, while the rest is generated by transportation, processing, and the refinement process [46]. The well-to-wheel (WTW) CO_2 emissions for kerosene fuel are modeled at 84.5 g $CO_{2\,eq}$/MJ with an 87% in combustion emissions [46]. Finally, the complete lifecycle of kerosene WTW is found by adding WWT to TTW CO_2 emissions of kerosene and LH_2 fuel sources from the extraction of crude oil or fuel to its combustion during flight.

The WTW for both H_2 combustion and the SOFC hybrid is estimated using green and gray hydrogen. Green hydrogen refers to the hydrogen produced via renewable energy, while gray hydrogen refers to the hydrogen produced using steam methane reformation without any greenhouse gas emissions capture. More than 95% of hydrogen produced today is produced using fossil fuels like natural gas and coal [47]. Meanwhile, green hydrogen requires a renewable energy-powered grid, which is not yet available in many parts of the world. However, most countries have plans to reach 100% renewable grids within the next 30–50 years [47]. The LCA estimation utilizes the Greenhouse Gases, Regulated Emissions, and Energy Use in Technologies (GREET) model to estimate the transportation lifecycle emissions via a mathematical framework that accounts for various pollutants such as CO_2 [48]. In addition, green hydrogen solar electrolysis is assumed to emit 41.29 g of $CO_{2\,eq}$/MJ for the full lifecycle, as referenced by Al-Breiki and Bicer [48]. Similarly, the gray hydrogen solar electrolysis full lifecycle is assumed to emit 75.6 g $CO_{2\,eq}$/MJ, as sourced by [49]. The mentioned LCA model

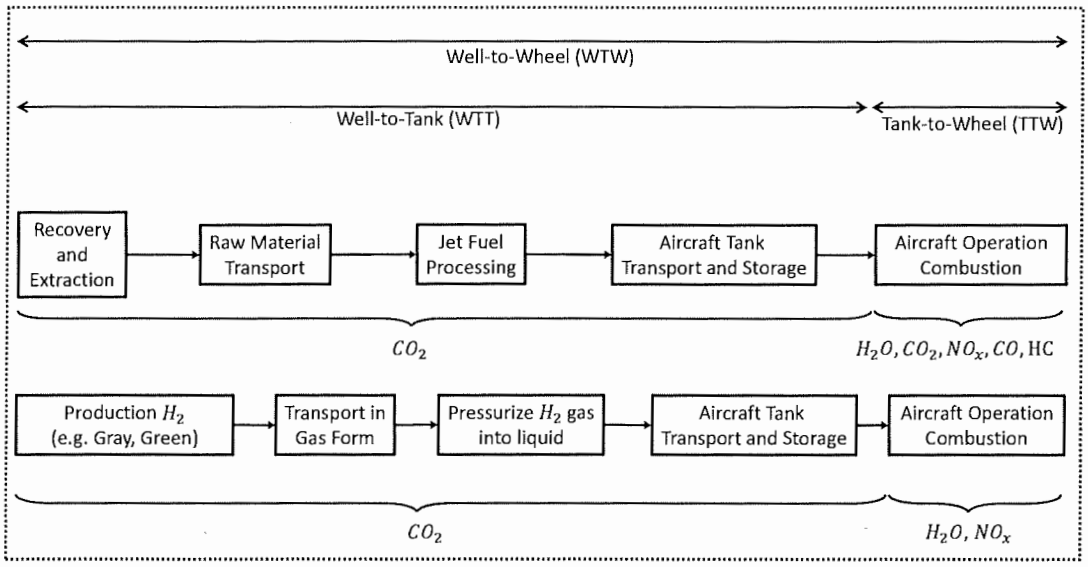

Fig. 7 Lifecycle assessment (LCA) boundary of Jet-A fuel (top) and LH_2 fuel (bottom).

does not include the production or life expectancy of lithium-ion batteries or the SOFC. The model is thus focused on the fuel WTW lifecycle. Although the environmental effects of producing those components are mainly from mining, not enough current data and research are available on the LCA of the SOFC hybrid system. TTW CO_2 emissions for all alternative fuel sources are modeled from the weight of the fuel inputted from the flight profile module, as discussed in Sec. II.D.

2. Cost Analysis

The change in fuel cost of implementing alternative fuel sources for one constant-range flight profile is determined to further analyze the tradeoffs of implementing a retrofit. The fuel burned per segment from the emissions module is utilized to model the fuel price per flight for this mission, in addition to the change in capital cost of the alternative fuel source. The cost of kerosene is determined by the full-service average kerosene Jet-A fuel price per gallon for the U.S. Western Pacific region for the current year. The price at the pump is assumed to already contain the production and transportation costs of kerosene. The cost of utilizing LH_2 for the proposed flight is modeled per segment in order to compare the change in fuel cost from a conventional kerosene-powered flight. The H_2 combustion change in fuel costs is estimated for both green and gray hydrogen. The cost of production for green hydrogen (electrolysis) was set at 5.5 USD/kg, while the production for gray carbon capture hydrogen was taken at 1.55 USD/kg, as suggested by Ajanovic et al. [50]. The cost liquefaction of both was set at 2.75 USD/kg, as suggested by Ghorbani et al. [51], while the cost of transportation was set at 5 USD/kg, as referenced by Hoelzen et al. [52].

In assessing the capital costs of retrofitting aircraft with hydrogen fuel systems, the focus is primarily on the integration of cryogenic tanks, estimated at $74.96 per kg of maximum LH_2 fuel capacity, following Yang et al. [53]. The initial cost analysis excludes heat exchanger costs based on the rationale that hydrogen combustion's expected thermal efficiency gains could diminish the necessity for comprehensive heat exchanger upgrades. Given their modular nature, heat exchangers are considered a lower priority in early evaluations, especially when compared to the substantial investments in cryogenic storage and fuel cell technologies. This approach prioritizes components critical to the retrofit's feasibility, with a detailed review of heat exchanger needs and other components like fuel lines, pumps, and valves deferred until further design specification in future analysis. The SOFC hybrid cost is modeled per segment for the purpose of comparison with LH_2 prices determined as stated above. In addition, the stack cost at a high production volume of SOFC can be assumed to be 238 USD per kilowatt of energy, as suggested by Xing et al. [54]. A 500 kW microturbine is assumed to have a midrange market price of 900 dollars per kilowatt following the California Distributed Energy Resources (DER) guide on microturbines and resourced by Chua et al. [55]. The lithium-ion battery cost is estimated to be 135 USD per kilowatt hour for the current year, as resourced by Varbanov et al. [56].

III. Methodology Demonstration for Alternative Fuel Retrofit on a Business Jet

The methodology developed in the previous section evaluates the potential to lower emissions for a single flight by utilizing a retrofit analysis. When compared to existing aircraft, business jets show a greater 34% net energy consumption reduction in emission values when utilizing H_2 fuel, as suggested by Nojoumi et al. [20]. Therefore, a business jet is chosen for this study since it has the greatest energy consumption reduction and the greatest potential to lower all emissions, including water vapor emissions. As global demand for private jet activity has risen by 7% in 2021, the implementation of the aforementioned methodology on the Cessna Citation 560 XLS+ business jet presents a potential opportunity for carbon mitigation [57]. A summary of key mission and performance specifications for the mentioned aircraft is found in Table 3.

The methodology presented in Sec. II is utilized to model the performance and emissions of the standard kerosene-powered Cessna Citation 560XLS+ in order to compare the tradeoffs resulting from a retrofitted H_2 combustion fuel and SOFC-hybrid-powered aircraft. In the flight profile module, these two alternative fuel power sources are examined for the same mission profile as the kerosene baseline procedure. The weight of the fuel required for this mission is determined for all three power plants as a function of heat energy available per unit weight of fuel, range, and other Breguet range equation parameters as shown in Sec. II.A. Such weights are utilized to design the tanks as stated in Sec. II.B and evaluated for feasibility in the CG module, as shown in Sec. II.C. A few passengers might be omitted if tank-sizing volume constraints are required to power the

Table 3 Cessna Citation 560 XLS+ performance specifications

Parameter	Value
Cruise range	3,889.2 km
Maximum number of passengers	9
Maximum speed limit	0.75 Mach
Maximum operating altitude	13,716 m
Thrust specific fuel consumption	0.045 kg/(N · h)

same mission, or a refueling stop might be added. A new fuel weight that accounts for such changes is then outputted into the emissions module. The flight emissions are then used to assess the lifecycle assessment and costs of implementing each retrofit. An overall analysis of the tradeoffs in performance and emissions by a retrofit methodology is output.

A. Analysis of Results

The conventional kerosene-, the H_2-combustion-, and the SOFC-hybrid-powered retrofit aircraft are all able to power the cruise mission specifications from Table 3. The fuel weights obtained from the flight profile module in Sec. II.A are seen in Table 4.

The power requirements and constraints of the H_2 combustion fuel and SOFC-hybrid-powered aircraft follow the energy assumptions described in Sec. II.A and are seen in Table 5. The power rating of the electric propulsion system is defined based on the maximum takeoff velocity of the aircraft and the thrust of the conventional aircraft. The battery size is defined as providing maximum thrust for 15 minutes. Such parameters and the fuel weight are used as design constraints in the tank configuration module.

The hydrogen cryogenic tanks are designed with insulation and altitude pressure as added design constraints. The resulting tank materials, properties, and characteristics are shown in Table 6. The design of the insulation maximizes flight temperature as specified in the thermal module in III.B.3. The tanks specified above are then evaluated for feasibility in the CG module. The three interior layout arrangements that satisfied the maximum and minimum CG envelope limits are seen in Fig. 8. The FAA minimum 30 cm aisle width regulation (for airplanes less than 10 passengers [32]) is exceeded for passenger comfort and evacuation regulations in all three configurations. The conventional arrangement of the Cessna 560 XLS+ is seen in Fig. 8a, with a forward refreshment center and an aft

Table 4 Fuel weights for cruise

Cruise weight	Jet-A, kg	H_2 combustion, kg	SOFC, kg
W_{start}	9,223.35	8,685.22	9,187.86
W_{end}	8,146.54	8,282.74	8,912.17
W_{fuel}	1,077.81	401.68	271.31

Table 5 Power and SOFC energy requirements

Parameter	Value
Thrust per engine, N	18,322
Maximum Takeoff velocity, km/h	230
Engine maximum power, kW	2,344.96
Energy required by H_2 combustion (MJ)	32,546.51
Energy, kW · h	9,040.70
Fuel cell power (75%), kW	1,758.72
Battery power (25%), kW	586.24
Battery size, kW · h	146.56
Cryocooler maximum power, kW	23.45

Table 6 Cryogenic LH_2 tanks

Parameter	Front tank	Aft tank		
Size	Small (6)	Large (1)	Medium (1)	Small (2)
r_{tot}, cm	25.60	60.20	23.08	20.07
L_{tot}, cm	157	271	271	271
V_{tot}, m^3	0.288	0.392	0.393	0.300
t_{in}, cm	0.089	0.211	0.081	0.070
Insulation thickness, cm	0.0079	0.008	0.008	0.008
W_t/W_f, %	23.8	23.5	24.1	24.1

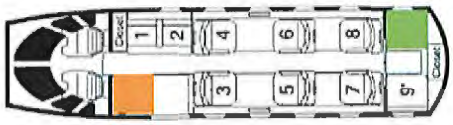

a) Jet-A

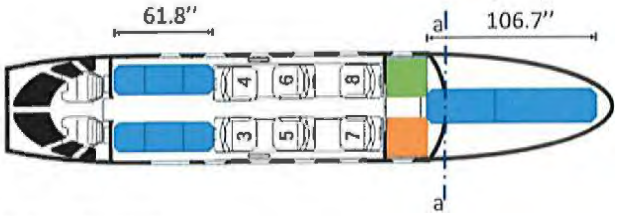

b) H_2-combustion

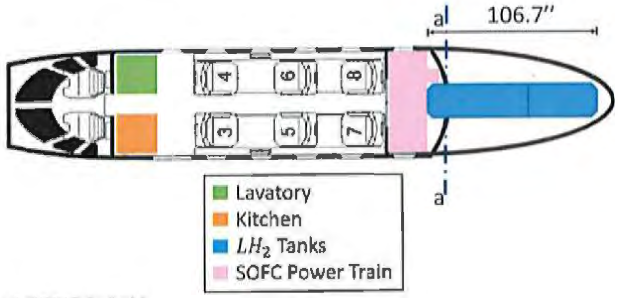

c) SOFC hybrid

Fig. 8 Interior layouts for retrofit analysis.

lavatory. The LH_2 tank design and layout result in six small tanks each of 157 cm distributed in the forward section of the cabin and four aft tanks, two of small size, one of midsize, and one of large size, all of 271 cm in length, as shown in Figs. 8b and 9. Such tank designs are subject to sizing and feasibility constraints and are seen in Table 6. However, passenger tables between seats 3 and 5 and 4 and 6 must be removed in order to fit the six small forward tanks. Nonetheless, the FAA minimum required first-class seat pitch of 96.5 cm is exceeded for all seats after such removal [32]. The H_2 combustion and SOFC layout required the removal of seats 1, 2, and 9, as well as the removal of the aft closet in order to fit the aft midsize LH_2 tank (25.4 cm) into section a-a of the cabin aft section, as shown in Figs. 8b and 8c. However, the SOFC required the shift of the forward lavatory and refreshment center since the aft section of the cabin is used to house the SOFC power train seen in pink in Fig. 8c.

The final design for both the retrofitted H_2 combustion and the SOFC hybrid both resulted in six passengers. For the H_2 combustion, these changes result in a 5% decrease in overall aircraft weight when compared to the conventional aircraft. For the SOFC, such changes result in a 0.4% decrease in mass when compared to conventional aircraft. This change in mass is observed due to the more energy-dense

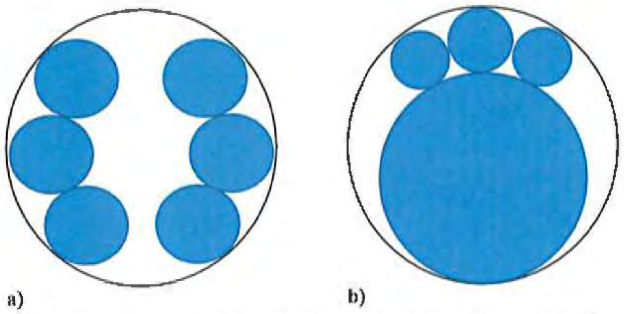

a) b)

Fig. 9 Cross section of fuselage: a) forward six small tanks; b) aft four tanks (one large, one medium, and two small tanks).

hydrogen, the choice of SOA materials, and the loss of three passengers, their seats, and luggage. The highest weights in the H_2 combustion aircraft are the empty weight and the weight of the passenger and bags, while the main weights in the SOFC are the empty weight and the fuel cell mass, as shown in Fig. 10. An H_2 combustion and SOFC-hybrid-powered aircraft can be designed where the same number of seats and cabin area are maintained. However, this would require a refueling stop and result in higher energy requirements and higher emissions for both the H_2 combustion and the SOFC hybrid aircraft.

As expected, H_2 combustion and the SOFC hybrid produce zero CO_2 emissions, as shown in Fig. 11. The figure also shows that kerosene fuel CO_2 and H_2O emissions are the highest during the cruise segments, with the second highest during the climb. Such a result is expected since emissions from these segments are dependent on how much time is spent while fuel is being burned. In comparison, higher emissions of CO and HC occur during idle and descent than CO_2 and H_2O emissions, due to incomplete combustion. H_2 combustion and the SOFC hybrid both result in higher water vapor emissions and could therefore have a likelihood of contrail formation. When compared to a conventional aircraft, the G-factor increases due to high vapor emissions and the possibility of the low static temperature of the exhaust. In addition, fuel cells can produce condensation phenomena at the Earth's surface if the weather is cold and close to frost. However, these are short-living phenomena that will disappear after a few seconds (outside of fog), and thus the term "contrail" should not be used for such a transient phenomenon.

As shown in Table 7, The NO_x emissions per passenger-km are 2.81×10^{-4} kg, 3.94×10^{-4} kg, and 2.12×10^{-4} kg for conventional, H_2 combustion, and SOFC hybrid aircraft, respectively. The water vapor (H_2O) emissions per passenger-km are 0.062, 0.255, and 0.137 kg for the conventional kerosene-powered aircraft, H_2 combustion, and SOFC-hybrid-powered aircraft, respectively. The contrailing of the water vapor emissions depends on the environment, combustion temperature, altitude, and mixing line "G" shown in Eq. (12). Thus, hydrogen combustion has the highest water vapor emissions per passenger-km, about four times more than conventional kerosene. To effectively mitigate contrail formation, a multifaceted approach is needed, considering the varying impacts of different powertrain technologies. Firstly, optimizing flight paths using real-time meteorological data can significantly reduce contrail formation, potentially by up to 20%, by avoiding areas prone to contrailing. Moreover, evading or reducing nighttime flights or flying at lower altitudes are possible solutions that must be critically assessed. Eliminating night flights would require a substantial increase in daytime airport and aircraft capacity, potentially inflating infrastructure costs significantly. Additionally, fuel consumption can increase by 10–15% when flying at lower altitudes compared to optimal cruise altitudes due to denser air at lower altitudes. Hence, addressing contrail formation requires balancing operational feasibility with environmental goals [20,58].

The full lifecycle of CO_2 results is categorized into two cases, as shown in Table 8. Case (i) stands for one flight with nine passengers

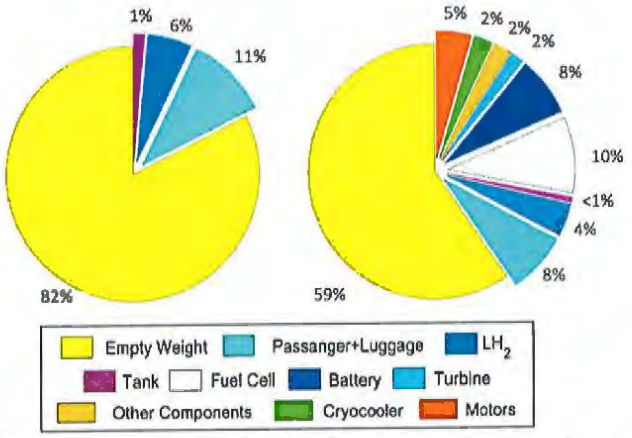

Fig. 10 Resulting fractional weights from implementing a retrofit on a H_2-combustion-powered (left) and an SOFC-hybrid-powered (right) Cessna Citation 560XLS+.

Table 7 NO_x and H_2O total emissions per passenger-km

Emission	Jet-A, kg/passenger-km	H_2, kg/passenger-km	SOFC hybrid, kg/passenger-km
NO_x	2.81×10^{-4}	3.94×10^{-4}	2.12×10^{-4}
H_2O	0.062	0.255	0.137

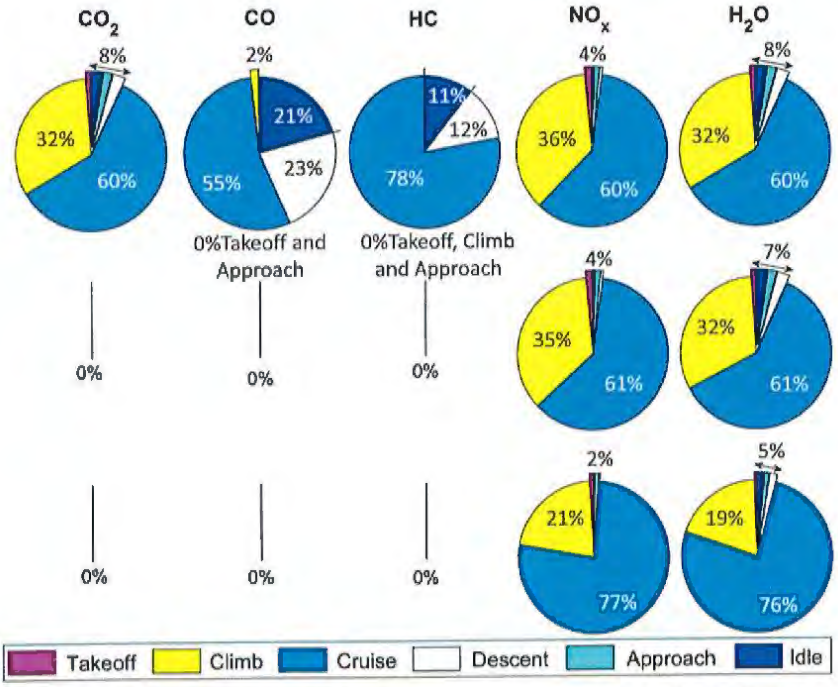

Fig. 11 CO_2, CO, HC, NO_x, and H_2O emissions per segment of conventional kerosene (top), H_2 combustion (middle), and retrofit SOFC-powered aircraft (bottom).

Table 8 CO_2 emissions for full lifecycle analysis of all configurations (kg/passenger-km)

Path	Case	Jet-A	Gray H_2	Green H_2	Gray SOFC	Green SOFC
Well-to-tank	(i)	0.0247	0.257	0.140	0.138	0.0755
CO_2	(ii)		0.343	0.187	0.184	0.101
Tank-to-wheel	(i)	0.162	0	0	0	0
CO_2	(ii)		0	0	0	0
Well-to-wheel	(i)	0.187	0.257	0.140	0.138	0.0755
CO_2	(ii)		0.343	0.187	0.184	0.101

for the conventional kerosene-powered aircraft, one flight with six passengers for the retrofit H_2-combustion-powered aircraft, and one flight with six passengers for the retrofit SOFC-hybrid-powered aircraft, whereas case (ii) models take an additional flight for the full lifecycle of the retrofit H_2 combustion and the retrofit SOFC hybrid aircraft. Such a model is obtained by keeping the same original amount of passengers (9) for the same range and adding an additional flight for both alternative fuel configurations. The results shown in Table 8 also show the full lifecycle as a function of the hydrogen sourcing production technique to compare emissions from both sourcing gray and green. As shown in Table 8, 86.8% of CO_2 emissions for the kerosene-powered aircraft happen during the combustion process in the TTW path of the fuel seen in Fig. 7 in Sec. II.E.1. However, if tank sizing constraints did not require a second flight for the H_2- and the SOFC-powered aircraft, the results would have been closer to the values obtained for all case (i) instances.

In case (ii), where an additional flight is required for the H_2- and SOFC-powered aircraft to carry the same number of passengers as the Jet-A-powered aircraft, the CO_2 emissions per passenger-km change significantly. The gray retrofit H_2-combustion-powered aircraft shows an 83.42% increase in WTW CO_2 emissions compared to the kerosene-powered aircraft. Surprisingly, the green retrofit H_2-combustion-powered aircraft does not show any change in WTW CO_2 emissions, remaining at a 0% difference. For the SOFC configurations, the gray retrofit SOFC hybrid shows a slight decrease of 1.60% in WTW CO_2 emissions, while the green retrofit SOFC hybrid demonstrates a more substantial decrease of 46% in WTW CO_2 emissions compared to the kerosene-powered aircraft. Such results arise from the carbon emissions during extraction, sourcing, transportation, and storage, as shown in the WTT path in Fig. 7 in Sec. II.E.1. These results highlight the nuanced environmental impact of transitioning to alternative fuel sources in aviation, especially when considering operational constraints like fuel tank sizing. While the adoption of green energy sources like the green H_2 and SOFC can lead to significant reductions in CO_2 emissions, operational factors such as the need for additional flights can offset these environmental benefits, as evidenced by the increased emissions for the gray retrofit H_2-combustion-powered aircraft in case (ii).

However, case (i) shows a significant reduction in WTW CO_2 emissions for three out of four configurations of the retrofit H_2 combustion aircraft (green) and the retrofit SOFC-powered aircraft (gray and green) when compared to the conventional kerosene-powered aircraft WTW CO_2 emissions. These percentages are −25.13% for the green retrofit H_2-combustion-powered aircraft, −26.20 and −59.63% for the gray and green retrofit SOFC-hybrid-powered aircraft, respectively. Lastly, the carbon emissions from the gray retrofit H_2-combustion-powered aircraft show a 37.43% increase compared to the conventional kerosene-powered aircraft WTW CO_2 emissions. This contrast in CO_2 emission reductions and increases across different fuel types emphasizes the complex interplay of factors in aviation's transition to greener alternatives. The significant decrease in CO_2 emissions for green H_2 and SOFC technologies highlights their potential in reducing the aviation sector's carbon footprint. However, the increase in emissions for the gray H_2 combustion aircraft underscores the challenges in selecting appropriate hydrogen sourcing methods. It reflects the necessity of considering the entire fuel production and consumption cycle when evaluating environmental impacts. The results from case (i) suggest that while alternative fuels can offer substantial environmental benefits, their adoption must be coupled with sustainable production methods to realize their full potential in reducing aviation's environmental impact.

To enhance the clarity in emission comparisons among different configurations, we assessed the Global Warming Potential (GWP) in terms of kg $CO_{2\,eq}$ emissions per passenger-km. This assessment considers GWP values over a 100 years derived from relevant literature [59–61]. The GWP factors employed in our analysis include CO_2 at a factor of 1, HC at 21, CO at 1.7, NO_x at 40, and H_2O at 0.059. Utilizing these factors, the TTW kg $CO_{2\,eq}$ emissions were calculated to be 0.177 kg $CO_{2\,eq}$/passenger-km for Jet-A aircraft, 0.0308 kg $CO_{2\,eq}$/passenger-km for single-flight H_2 combustion, and 0.0165 kg CO_{2eq}/passenger-km for single-flight SOFC hybrid system. It is crucial to recognize that these values may vary depending on numerous factors, including the geographic location of the flight. These assumptions are specific to North American airspace, where the reference flight is conducted. The TTW emissions associated with hydrogen fuel consumption exhibit significantly lower GWP across both configurations when compared to the combustion of kerosene. Incorporating WTT CO_2 emissions, as detailed in Table 8, reveals that Jet-A fuel possesses a GWP of 0.217 kg $CO_{2\,eq}$/passenger-km, whereas green hydrogen demonstrates a GWP of 0.171 kg $CO_{2\,eq}$/passenger-km. Additionally, green SOFC technology presents a GWP of 0.092 kg $CO_{2\,eq}$/ passenger-km.

The integration of SOFC in aviation, while promising for emissions reduction, is constrained by several technical and operational limitations. Firstly, the lifespan of SOFCs in aviation contexts is a critical issue. SOFCs exhibit degradation rates of 1–3% per 1000 operating hours, depending on operation, whereby less than 0.5%/1000 h are required for economic efficiency [62,63]. Stationary power systems are commercially available today with stacks that exhibit very long lifetimes in the range of 40,000–70,000 h [64], but for more highly dynamic and more rigorous transport application, SOFC lifetime is expected to be 4000–5000 h after intense degradation [65,66], contrasting with the average lifespan of conventional aircraft engines like the Pratt & Whitney Canada PW545C, which can exceed 6000 h before an engine overhaul is required [33]. Hence, more frequent replacement of the SOFC is expected to increase lifecycle emissions costs. The production of a 1 kW planar SOFC CHP system is estimated to result in the emission of approximately 700–950 kg of CO_2. These impacts are further amplified when accounting for the production of replacement stacks [67]. This discrepancy in lifespan necessitates more frequent replacements for SOFCs, thereby imposing higher lifecycle emissions and maintenance costs.

Additionally, SOFCs' sensitivity to fuel impurities, especially when powered by gray hydrogen containing contaminants like sulfur or carbon monoxide, can degrade cell performance and reduce efficiency. These impurities can poison the Ni-based anode, leading to a decrease in the electrochemically active surface area and a deterioration of cell performance. A 1% contamination by volume can decrease cell lifespan by up to 10% [68,69]. Moreover, fast temperature changes during flight pose durability challenges. The thermal management of SOFC systems, which must maintain a constant operating temperature for maximum performance, may face difficulties as a result of this temperature variation [70]. Additionally, the impact of aircraft vibrations on SOFC integrity is notable. Vibrations can lead to microcracks in the cell structure, affecting performance. Under conditions of intense vibration, the ceramic materials used in SOFCs can exhibit brittleness, making them prone to mechanical breakdowns, especially at high temperatures. Electrochemically, microcracks in SOFCs impair performance by disrupting the electrolyte layer's ability to conduct oxygen ions, thus decreasing ionic conductivity and electrochemical efficiency. These cracks also allow fuel and oxidant gases to mix, reducing fuel efficiency and potentially causing cell failure. Furthermore, microcracks in the electrode layers reduce the active surface area, further diminishing the cell's electrochemical performance [71]. Thermal management also presents a substantial challenge. SOFCs operate at high temperatures, necessitating advanced cooling systems

Table 9 Total fuel cost per segment per passenger-km

Segment	Case	Jet-A, $	Gray H_2, $	Green H_2, $	SOFC H_2 gray, $	SOFC H_2 green, $
Takeoff ($\times 10^{-3}$)	(i)	1.26	2.75	3.84	0.892	1.25
Climb ($\times 10^{-3}$)	(i)	38.3	83.3	116	27.1	37.8
Cruise	(i)	70.6	160	224	108	151
Descent ($\times 10^{-3}$)	(i)	3.15	6.86	9.58	2.23	3.12
Approach ($\times 10^{-3}$)	(i)	2.16	4.71	6.58	1.53	2.14
Taxi/idle ($\times 10^{-3}$)	(i)	2.90	6.31	8.83	2.05	2.87
Entire flight ($\times 10^{-3}$)	(i)	118	264	369	142	198
Entire flight ($\times 10^{-3}$)	(ii)		352	492	189	264
Total fuel cost for mission	(i)	4,143.18	6,161.55	8,612.92	3,310.33	4,627.34
	(ii)		12,323.10	17,225.84	6,620.66	9,254.68

that increase weight and complexity. Controlling the heat output of SOFCs in an aircraft's confined space is crucial. Present thermal management solutions can restrict SOFC power output to the kW scale, which falls short of the requirements for medium-sized aircraft. These limitations underscore the necessity for considerable advancements in SOFC technology and infrastructure to make them a feasible option for aircraft applications [72].

Two cases were evaluated following the same approach as the lifecycle emissions for cases (i) and (ii). From an economic perspective, significant changes in fuel costs per passenger-km result from replacing kerosene with alternative fuel sources. In case (i), as shown in Table 9, the fuel cost per passenger-km for gray H_2 combustion is 123.73% higher than kerosene, while green H_2 shows an even greater increase of 212.71% due to the higher cost of green H_2 production. The SOFC gray H_2 configuration offers a 20.34% increase in fuel cost per passenger-km compared to kerosene, while the SOFC green H_2 configuration sees an increase of 67.80%.

In case (ii), where two flights are required to carry the same number of passengers, the fuel costs per passenger-km change more significantly. The SOFC gray H_2 shows a 198.31% increase in fuel cost per passenger-km, while green H_2 shows a staggering 316.95% increase when compared to kerosene for case (i). The SOFC hybrid configurations also exhibit increases in fuel costs per passenger-km, with the gray SOFC hybrid showing a 60.17% increase and the green SOFC hybrid showing a 123.73% increase compared to kerosene for case (i).

The change in capital cost for purchasing the SOFC hybrid includes a total of 919,497.27 USD for the cryogenic tanks plus the SOFC power train, while the change in capital costs for the H_2 combustion aircraft is 49,661.50 USD from the cryogenic tanks. Additionally, when examining the "total fuel cost for mission" as presented in Table 9, a significant economic implication emerges for both cases. In case (i), the total fuel cost for alternative fuels ranges from \$3310.33 to \$8612.92, with the green H_2 being the most expensive, highlighting the premium associated with greener options. Conversely, in case (ii), the total fuel cost escalates substantially for the H_2 and SOFC configurations due to the requirement of an additional flight, with costs ranging from \$6620.66 to \$17,225.84, thereby emphasizing the economic impact of operational constraints in the adoption of alternative fuels. These cost changes highlight the economic challenges associated with transitioning to alternative fuels in aviation. While some configurations show significant increases in fuel costs, particularly in scenarios requiring additional flights, they reflect the current state of technology and the premium associated with greener fuel options. This underscores the importance of considering both environmental and economic factors in the adoption of alternative fuels in the aviation industry.

IV. Conclusions

The proposed methodology models the performance, emissions, lifecycle, and costs of a retrofitted H_2 combustion and a retrofitted SOFC-hybrid-powered aircraft. Such methodology consists of a constant range and airframe analysis to design LH_2 fuel tanks that satisfy insulation, sizing, CG, and power constraints. The interior layout analysis results in a 5 and 0.4% decrease in takeoff weight for the H_2 combustion and SOFC hybrid aircraft, respectively. However, the resulting mass change is achieved at the cost of removing a few passengers and their luggage to account for cryogenic tank sizing and weight constraints for the same range. Therefore, neither H_2 combustion nor the SOFC hybrid aircraft are able to carry the same number of passengers for the same range as the kerosene-powered aircraft. Although kerosene-powered aircraft can transport a greater number of passengers per trip, carbon emissions are higher since conventional kerosene combustion has the highest WTW CO_2 kg emissions of 6546 kg per flight. However, for kg CO_2 per passenger-km, gray H_2 combustion aircraft surprisingly result in the highest WTW CO_2 emissions. Nevertheless, a great advantage for potential carbon mitigation arises from utilizing hydrogen alternative fuels since kerosene combustion also produces other greenhouse gas emissions besides NO_x, CO_2, and H_2O that all systems share. The NO_x emissions per passenger-km are highest in H_2 combustion aircraft and lower in kerosene and SOFC hybrid aircraft, consecutively.

In terms of WTW CO_2 emissions per passenger-km, the study reveals varied impacts depending on the fuel type and operational scenario. Case (i) shows that green hydrogen and SOFC technologies significantly reduce CO_2 emissions in aviation, with reductions of 25.13 and 59.63%, respectively, compared to conventional kerosene. However, the gray H_2 combustion aircraft increases emissions by 37.43%. However, other greenhouse emissions must be evaluated when comparing the SOFC hybrid to the H_2 combustion. H_2O TTW emissions are highest for the H_2 combustion aircraft and therefore have a likelihood for contrail formation. Addressing contrail formation is crucial given its radiative forcing impact, which is comparable in magnitude to CO_2 emissions from kerosene combustion [73]. However, alternatives like avoiding night-time flights or flying at lower altitudes must be evaluated against practical and economic constraints. For instance, restricting night flights significantly increases demand for daytime airport and aircraft capacity, potentially escalating infrastructure costs. Moreover, lower-altitude flights could lead to increased fuel consumption and emissions, offsetting the benefits of reduced contrail formation. This necessitates a balanced approach where strategies are tailored to optimize both environmental impact and operational feasibility. Further exploration into efficient flight routing, advanced aircraft designs, and alternative fuels could provide more viable solutions for managing contrail effects without disproportionate cost implications. The economic analysis also reveals significant increases in fuel costs per passenger-km for both H_2 combustion and SOFC configurations, compared to kerosene. The most notable is green H_2 shows a 212.71% increase for the green H_2 combustion variant, which is likely due to the higher production costs associated with green hydrogen. Meanwhile, the SOFC gray H_2 configuration offers the cheapest change in price with a 20.34% increase in fuel cost per passenger-km due to the lower cost of gray hydrogen and the higher efficiency of the system. However, a more expensive one-time capital cost of \$919,497.27 comes from purchasing the SOFC power train. Such is a potential tradeoff that aids carbon mitigation in the near future at the cost of omitting a few passengers for the same range.

Moreover, in our exploration of retrofitting business jets with alternative propulsion systems, we have carefully considered a range of crucial factors, such as the aircraft's weight, operational range,

cabin size, and engine types such as turbofan, turbojet, and turboprop. The focus of our study, primarily on the Cessna Citation XLS+, has yielded a methodology robust and versatile enough to be applied across various aircraft categories and engine types. However, it is imperative to also account for the specific maintenance requirements and operational efficiencies of different aircraft models in any comprehensive retrofitting strategy. Our research, while detailed for the Cessna Citation XLS+, provides a foundation for subsequent studies. The findings indicate that, generally, medium-sized business jets with similar cabin sizes and power requirements in the same range (around 13 cubic meters and 2.3 MW, respectively) are likely to be suitable candidates for similar retrofitting processes. Business jets of similar size and lower power requirements should particularly expect positive retrofitting results. Importantly, the analysis we conducted also suggests the need to validate the generalizability of our success with the Cessna Citation XLS+ to other similar medium-sized, nine-seater business jets. This validation is crucial, as it will confirm the broader applicability and potential effectiveness of our retrofitting methodologies across a wider array of aircraft within the aviation industry.

The results presented in the retrofit, cost, and emissions analysis illustrate the complex balance between environmental benefits and economic considerations in the aviation sector's transition to alternative fuels. While alternative fuels like hydrogen and SOFC technologies offer potential reductions in CO_2 emissions, their economic viability and the operational adjustments required (such as passenger capacity reductions for the same flight range) must be carefully considered. The methodology presented is adaptable to various aircraft categories and engine types, but its broader application requires an assessment of these multifaceted variables.

References

[1] Owen, B., Lee, D. S., and Lim, L., "Flying into the Future: Aviation Emissions Scenarios to 2050," *Environmental Science & Technology*, Vol. 44, No. 7, 2010, pp. 2255–2260. https://doi.org/10.1021/es902530z

[2] Voskuijl, M., Van Bogaert, J., and Rao, A. G., "Analysis and Design of Hybrid Electric Regional Turboprop Aircraft," *Council of European Aerospace Societies Aeronautical Journal*, Vol. 9, March 2018, pp. 15–25. https://doi.org/10.1007/s13272-017-0272-1

[3] Adu-Gyamfi, B. A., and Good, C., "Electric Aviation: A Review of Concepts and Enabling Technologies," *Transportation Engineering*, Vol. 9, Sept. 2022, Paper 100134. https://doi.org/10.1016/j.treng.2022.100134

[4] Adler, E. J., and Martins, J. R., "Hydrogen-Powered Aircraft: Fundamental Concepts, Key Technologies, and Environmental Impacts," *Progress in Aerospace Sciences*, Vol. 141, Aug. 2023, Paper 100922. https://doi.org/10.1016/j.paerosci.2023.100922

[5] Massaro, M. C., Biga, R., Kolisnichenko, A., Marocco, P., Monteverde, A. H. A., and Santarelli, M., "Potential and Technical Challenges of On-Board Hydrogen Storage Technologies Coupled with Fuel Cell Systems for Aircraft Electrification," *Journal of Power Sources*, Vol. 555, Jan. 2023, Paper 232397. https://doi.org/10.1016/j.jpowsour.2022.232397

[6] Abbe, G., and Smith, H., "Technological Development Trends in Solar-Powered Aircraft Systems," *Renewable and Sustainable Energy Reviews*, Vol. 60, July 2016, pp. 770–783. https://doi.org/10.1016/j.rser.2016.01.053

[7] Wang, M., Dewil, R., Maniatis, K., Wheeldon, J., Tan, T., Baeyens, J., and Fang, Y., "Biomass-Derived Aviation Fuels: Challenges and Perspective," *Progress in Energy and Combustion Science*, Vol. 74, Sept. 2019, pp. 31–49. https://doi.org/10.1016/j.pecs.2019.04.004

[8] Nicolay, S., Karpuk, S., Liu, Y., and Elham, A., "Conceptual Design and Optimization of a General Aviation Aircraft with Fuel Cells and Hydrogen," *International Journal of Hydrogen Energy*, Vol. 46, No. 64, 2021, pp. 32,676–32,694. https://doi.org/10.1016/j.ijhydene.2021.07.127

[9] Palladino, V., Bartoli, N., Pommier-Budinger, V., Bénard, E., Schmollgruber, P., and Jordan, A., "Optimization of a Hydrogen-Based Hybrid Propulsion System Under Aircraft Performance Constraints," *Chinese Journal of Aeronautics*, Vol. 36, No. 5, 2023, pp. 41–56. https://doi.org/10.1016/j.cja.2023.02.019

[10] Abu Kasim, A., Chan, M., and Marek, E., "Performance and Failure Analysis of a Retrofitted Cessna Aircraft with a Fuel Cell Power System Fuelled with Liquid Hydrogen," *Journal of Power Sources*, Vol. 521, Feb. 2022, Paper 230987. https://doi.org/10.1016/j.jpowsour.2022.230987

[11] Rupiper, L. N., Skabelund, B. B., Ghotkar, R., and Milcarek, R. J., "Impact of Fuel Type on the Performance of a Solid Oxide Fuel Cell Integrated with a Gas Turbine," *Sustainable Energy Technologies and Assessments*, Vol. 51, June 2022, Paper 101959. https://doi.org/10.1016/j.seta.2022.101959

[12] Seitz, A., Nickl, M., Troeltsch, F., and Ebner, K., "Initial Assessment of a Fuel Cell—Gas Turbine Hybrid Propulsion Concept," *Aerospace*, Vol. 9, No. 2, 2022, p. 68. https://doi.org/10.3390/aerospace9020068

[13] Liu, H., Qin, J., Xiu, X., Ha, C., and Dong, P., "Comparative Study of Fuel Types on Solid Oxide Fuel Cell—Gas Turbine Hybrid System for Electric Propulsion Aircraft," *Fuel*, Vol. 347, Sept. 023, Paper 128426. https://doi.org/10.1016/j.fuel.2023.128426

[14] Collins, J. M., and McLarty, D., "All-Electric Commercial Aviation with Solid Oxide Fuel Cell-Gas Turbine-Battery Hybrids," *Applied Energy*, Vol. 265, May 2020, Paper 114787. https://doi.org/10.1016/j.apenergy.2020.114787

[15] Tiwari, S., Pekris, M. J., and Doherty, J. J., "A Review of Liquid Hydrogen Aircraft and Propulsion Technologies," *International Journal of Hydrogen Energy*, Vol. 57, Feb. 2024, pp. 1174–1196. https://doi.org/10.1016/j.ijhydene.2023.12.263

[16] Baroutaji, A., Wilberforce, T., Ramadan, M., and Olabi, A. G., "Comprehensive Investigation on Hydrogen and Fuel Cell Technology in the Aviation and Aerospace Sectors," *Renewable and Sustainable Energy Reviews*, Vol. 106, May 2019, pp. 31–40. https://doi.org/10.1016/j.rser.2019.02.022

[17] Rivard, E., Trudeau, M., and Zaghib, K., "Hydrogen Storage for Mobility: A Review," *Materials*, Vol. 12, No. 12, 2019. https://doi.org/10.3390/ma12121973

[18] Prewitz, M., Bardenhagen, A., and Beck, R., "Hydrogen as the Fuel of the Future in Aircrafts—Challenges and Opportunities," *International Journal of Hydrogen Energy*, Vol. 45, No. 46, 2020, pp. 25,378–25,385. https://doi.org/10.1016/j.ijhydene.2020.06.238

[19] Gössling, S., and Dolnicar, S., "Review of Air Travel Behavior and Climate Change," *Wiley Interdisciplinary Reviews: Climate Change*, Vol. 14, No. 1, 2023, Paper e802. https://doi.org/10.1002/wcc.802

[20] Nojoumi, H., Dincer, I., and Naterer, G., "Greenhouse Gas Emissions Assessment of Hydrogen and Kerosene-Fueled Aircraft Propulsion," *International Journal of Hydrogen Energy*, Vol. 34, No. 3, 2009, pp. 1363–1369. https://doi.org/10.1016/j.ijhydene.2008.11.017

[21] Barton, D. I., Hall, C. A., and Oldfield, M. K., "Design of a Hydrogen Aircraft for Zero Persistent Contrails," *Aerospace*, Vol. 10, No. 8, 2023, p. 688. https://doi.org/10.3390/aerospace10080688

[22] Liu, Y., Sun, X., Sethi, V., Nalianda, D., Li, Y.-G., and Wang, L., "Review of Modern Low Emissions Combustion Technologies for Aero Gas Turbine Engines," *Progress in Aerospace Sciences*, Vol. 94, Oct. 2017, pp. 12–45. https://doi.org/10.1016/j.paerosci.2017.08.001

[23] Stefan, E., Talic, B., Larring, Y., Gruber, A., and Peters, T. A., "Materials Challenges in Hydrogen-Fuelled Gas Turbines," *International Materials Reviews*, Vol. 67, No. 5, 2022, pp. 461–486. https://doi.org/10.1080/09506608.2021.1981706

[24] Ahluwalia, R., Hua, T., Peng, J.-K., Lasher, S., McKenney, K., Sinha, J., and Gardiner, M., "Technical Assessment of Cryo-Compressed Hydrogen Storage Tank Systems for Automotive Applications," *International Journal of Hydrogen Energy*, Vol. 35, No. 9, 2011, pp. 4171–4184. https://doi.org/10.1016/j.ijhydene.2010.02.074

[25] Wilson, J. A., Wang, Y., Carroll, J., Raush, J., Arkenberg, G., Dogdibegovic, E., Swartz, S., Daggett, D., Singhal, S., and Zhou, X.-D., "Hybrid Solid Oxide Fuel Cell/Gas Turbine Model Development for Electric Aviation," *Energies*, Vol. 15, No. 8, 2022, Paper 2885. https://doi.org/10.3390/en15082885

[26] Scholz, A. E., Michelmann, J., and Hornung, M., "Fuel Cell Hybrid-Electric Aircraft: Design, Operational, and Environmental Impact," *Journal of Aircraft*, Vol. 60, No. 1, 2022, pp. 606–622. https://doi.org/10.2514/1.C036952

[27] Tornabene, R., Wang, X., Steffen, C. J., Jr., and Freeh, J., "Development of Parametric Mass and Volume Models for an Aerospace SOFC/Gas Turbine Hybrid System," *Proceedings of the ASME Turbo Expo 2005: Power for Land, Sea, and Air, Turbo Expo 2005*, Vol. 5, American Soc.

of Mechanical Engineers, Fairfield, NJ, 2005, pp. 135–144. https://doi.org/10.1115/GT2005-68334

[28] Haran, K. S., Kalsi, S., Arndt, T., Karmaker, H., Badcock, R., Buckley, B., Haugan, T., Izumi, M., Loder, D., Bray, J. W., et al., "High Power Density Superconducting Rotating Machines—Development Status and Technology Roadmap," *Superconductor Science and Technology*, Vol. 30, No. 12, 2017, Paper 123002. https://doi.org/10.1088/1361-6668/aa833e

[29] Winnefeld, C., Kadyk, T., Bensmann, B., Krewer, U., and Hanke-Rauschenbach, R., "Modelling and Designing Cryogenic Hydrogen Tanks for Future Aircraft Applications," *Energies*, Vol. 11, No. 1, 2018, p. 105. https://doi.org/10.3390/en11010105

[30] Colozza, A. J., and Kohout, L., "Hydrogen Storage for Aircraft Applications Overview," NASA CR-2002-211867, Sept. 2002.

[31] Hamel, C., Sassi, A., Botez, R., and Dartigues, C., "Cessna Citation X Aircraft Global Model Identification from Flight Tests," *SAE International Journal of Aerospace*, Vol. 6, No. 1, 2013, pp. 106–114. https://doi.org/10.4271/2013-01-2094

[32] Takahashi, T., *Aircraft Performance and Sizing, Volume I: Fundamentals of Aircraft Performance*, Aerospace Engineering Collection, Momentum Press, New York, 2017.

[33] Shevell, R. S., *Fundamental Principles of Flight*, 2nd ed., Prentice–Hall, Hoboken, NJ, 1989.

[34] Palies, P. P., "Hydrogen Thermal-Powered Aircraft Combustion and Propulsion System," *Journal of Engineering for Gas Turbines and Power*, Vol. 144, No. 10, 2022, Paper 101007. https://doi.org/10.1115/1.4055270

[35] Ocko, I. B., and Hamburg, S. P., "Climate Consequences of Hydrogen Emissions," *Atmospheric Chemistry and Physics*, Vol. 22, No. 14, 2022, pp. 9349–9368. https://doi.org/10.5194/acp-22-9349-2022

[36] Wayson, R. L., Fleming, G. G., and Iovinelli, R., "Methodology to Estimate Particulate Matter Emissions from Certified Commercial Aircraft Engines," *Journal of the Air & Waste Management Association*, Vol. 59, No. 1, 2009, pp. 91–100. https://doi.org/10.3155/1047-3289.59.1.91

[37] Therkelsen, P., Werts, T., McDonell, V., and Samuelsen, S., "Analysis of NOx Formation in a Hydrogen-Fueled Gas Turbine Engine," *Journal of Engineering for Gas Turbines and Power*, Vol. 131, No. 3, 2009, Paper 031507. https://doi.org/10.1115/1.3028232

[38] Khan, M. A. H., Brierley, J., Tait, K. N., Bullock, S., Shallcross, D. E., and Lowenberg, M. H., "The Emissions of Water Vapour and NOx from Modelled Hydrogen-Fuelled Aircraft and the Impact of NOx Reduction on Climate Compared with Kerosene-Fuelled Aircraft," *Atmosphere*, Vol. 13, No. 10, 2022, Paper 1660. https://doi.org/10.3390/atmos13101660

[39] Ingenito, A., Agresta, A., Andriani, R., and Gamma, F., "NOx Reduction Strategies for High Speed Hydrogen Fuelled Vehicles," *International Journal of Hydrogen Energy*, Vol. 40, No. 15, 2015, pp. 5186–5196. https://doi.org/10.1016/j.ijhydene.2015.02.100

[40] Stettler, M. E. J., Koudis, G. S., Hu, S. J., Majumdar, A., and Ochieng, W. Y., "The Impact of Single Engine Taxiing on Aircraft Fuel Consumption and Pollutant Emissions," *Aeronautical Journal*, Vol. 122, No. 1258, 2018, pp. 1967–1984. https://doi.org/10.1017/aer.2018.117

[41] Di Mascio, P., Corazza, M. V., Rosa, N. R., and Moretti, L., "Optimization of Aircraft Taxiing Strategies to Reduce the Impacts of Landing and Take-Off Cycle at Airports," *Sustainability*, Vol. 14, No. 15, 2022, Paper 9692. https://doi.org/10.3390/su14159692

[42] Khardi, S., "Optimization of Aircraft Fuel Consumption and Reduction of Pollutant Emissions: Environmental Impact Assessment," *Advances in Aircraft and Spacecraft Science*, Vol. 1, No. 3, 2014, pp. 311–330. https://doi.org/10.12989/aas.2014.1.3.311

[43] Gierens, K., "Theory of Contrail Formation for Fuel Cells," *Aerospace*, Vol. 8, No. 6, 2021, p. 164. https://doi.org/10.3390/aerospace8060164

[44] Spangenberg, D., Minnis, P., Bedka, S., Palikonda, R., Duda, D., and Rose, F., "Contrail Radiative Forcing over the Northern Hemisphere from 2006 Aqua MODIS Data," *Geophysical Research Letters*, Vol. 40, No. 3, 2013, pp. 595–600. https://doi.org/10.1002/grl.50168

[45] Koroneos, C., Dompros, A., Roumbas, G., and Moussiopoulos, N., "Advantages of the Use of Hydrogen Fuel as Compared to Kerosene," *Resources, Conservation and Recycling*, Vol. 44, No. 2, 2005, pp. 99–113. https://doi.org/10.1016/j.resconrec.2004.09.004

[46] Detsios, N., Theodoraki, S., Maragoudaki, L., Atsonios, K., Grammelis, P., and Orfanoudakis, N. G., "Recent Advances on Alternative Aviation Fuels/Pathways: A Critical Review," *Energies*, Vol. 16, No. 4, 2023, Paper 1904. https://doi.org/10.3390/en16041904

[47] Kakoulaki, G., Kougias, I., Taylor, N., Dolci, F., Moya, J., and Jäger-Waldau, A., "Green Hydrogen in Europe—A Regional Assessment: Substituting Existing Production with Electrolysis Powered by Renewables," *Energy Conversion and Management*, Vol. 228, Jan. 2021, Paper 113649. https://doi.org/10.1016/j.enconman.2020.113649

[48] Al-Breiki, M., and Bicer, Y., "Comparative Life Cycle Assessment of Sustainable Energy Carriers Including Production, Storage, Overseas Transport, and Utilization," *Journal of Cleaner Production*, Vol. 279, Jan. 2021, Paper 123481. https://doi.org/10.1016/j.jclepro.2020.123481

[49] Howarth, R. W., and Jacobson, M. Z., "How Green is Blue Hydrogen?" *Energy Science & Engineering*, Vol. 9, No. 10, 2021, pp. 1676–1687. https://doi.org/10.1002/ese3.956

[50] Ajanovic, A., Sayer, M., and Haas, R., "The Economics and the Environmental Benignity of Different Colors of Hydrogen," *International Journal of Hydrogen Energy*, Vol. 47, No. 57, 2022, pp. 24,136–24,154. https://doi.org/10.1016/j.ijhydene.2022.02.094

[51] Ghorbani, B., Zendehboudi, S., Saady, N. M. C., Duan, X., and Albayati, T. M., "Strategies To Improve the Performance of Hydrogen Storage Systems by Liquefaction Methods: A Comprehensive Review," *American Chemical Society Omega*, Vol. 8, No. 21, 2023, pp. 18,358–18,399. https://doi.org/10.1021/acsomega.3c01072

[52] Hoelzen, J., Silberhorn, D., Zill, T., Bensmann, B., and Hanke-Rauschenbach, R., "Hydrogen-Powered Aviation and Its Reliance on Green Hydrogen Infrastructure—Review and Research Gaps," *International Journal of Hydrogen Energy*, Vol. 47, No. 5, 2022, pp. 3108–3130. https://doi.org/10.1016/j.ijhydene.2021.10.239

[53] Yang, B., Mane, M., and Crossley, W. A., "An Approach to Evaluate Fleet Level CO2 Impact of Introducing Liquid-Hydrogen Aircraft to a World-Wide Network," *AIAA Aviation and Aeronautics Forum and Exposition*, AIAA Paper 2022-3313, 2022. https://doi.org/10.2514/6.2022-3313

[54] Xing, H., Stuart, C., Spence, S., and Chen, H., "Fuel Cell Power Systems for Maritime Applications: Progress and Perspectives," *Sustainability*, Vol. 13, No. 3, 2021, Paper 1213. https://doi.org/10.3390/su13031213

[55] Chua, K., Yang, W., Er, S., and Ho, C., "Sustainable Energy Systems for a Remote Island Community," *Applied Energy*, Vol. 113, Jan. 2014, pp. 1752–1763. https://doi.org/10.1016/j.apenergy.2013.09.030

[56] Varbanov, P. S., Wang, B., Klemeš, J. J., Kabli, M. R., Shahzad, K., and Ocłoń, P., "Municipal Power Plan Optimisation Accounting for Environmental Footprints," *Energy Conversion and Management*, Vol. 254, Feb. 2022, Paper 115296. https://doi.org/10.1016/j.enconman.2022.115296

[57] Sobieralski, J. B., and Mumbower, S., "Jet-Setting During COVID-19: Environmental Implications of the Pandemic-Induced Private Aviation Boom," *Transportation Research Interdisciplinary Perspectives*, Vol. 13, March 2022, Paper 100575. https://doi.org/10.1016/j.trip.2022.100575

[58] Khan, M. A. H., Brierley, J., Tait, K. N., Bullock, S., Shallcross, D. E., and Lowenberg, M. H., "The Emissions of Water Vapour and NOx from Modelled Hydrogen-Fuelled Aircraft and the Impact of NOx Reduction on Climate Compared with Kerosene-Fuelled Aircraft," *Atmosphere*, Vol. 13, No. 10, 2022, Paper 1660. https://doi.org/10.3390/atmos13101660

[59] Fuglestvedt, J., Shine, K., Berntsen, T., Cook, J., Lee, D., Stenke, A., Skeie, R., Velders, G., and Waitz, I., "Transport Impacts on Atmosphere and Climate: Metrics," *Atmospheric Environment*, Vol. 44, No. 37, 2010, pp. 4648–4677. https://doi.org/10.1016/j.atmosenv.2009.04.044

[60] Skowron, A., Lee, D. S., and De León, R. R., "Variation of Radiative Forcings and Global Warming Potentials from Regional Aviation NOx Emissions," *Atmospheric Environment*, Vol. 104, March 2015, pp. 69–78. https://doi.org/10.1016/j.atmosenv.2014.12.043

[61] Jungbluth, N., and Meili, C., "Recommendations for Calculation of the Global Warming Potential of Aviation Including the Radiative Forcing Index," *International Journal of Life Cycle Assessment*, Vol. 24, March 2019, pp. 404–411. https://doi.org/10.1007/s11367-018-1556-3

[62] Königshofer, B., Boškoski, P., Nusev, G., Koroschetz, M., Hochfellner, M., Schwaiger, M., Juričić, Đani, Hochenauer, C., and Subotić, V.,

"Performance Assessment and Evaluation of SOC Stacks Designed for Application in a Reversible Operated 150 kW rSOC Power Plant," *Applied Energy*, Vol. 283, Feb. 2021, Paper 116372. https://doi.org/10.1016/j.apenergy.2020.116372

[63] Eichhorn Colombo, K. W., Schütz, P., and Kharton, V. V., "Reliability Analysis for a Multi-Stack Solid Oxide Fuel Cell System Subject to Operation Condition-Dependent Degradation," *Journal of Quality in Maintenance Engineering*, Vol. 28, No. 1, 2022, pp. 102–130. https://doi.org/10.1108/JQME-04-2020-0021

[64] Nakajo, A., Mueller, F., McLarty, D., Brouwer, J., and Favrat, D., "The Effects of Dynamic Dispatch on the Degradation and Lifetime of Solid Oxide Fuel Cell Systems," *Journal of the Electrochemical Society*, Vol. 158, No. 11, 2011, Paper B1329. https://doi.org/10.1149/2.032111jes

[65] Ido, A., Asano, K., Morita, H., Yamamoto, T., and Mugikura, Y., "Degradation Analysis of SOFC Performance (1)—Severe Operation with High Fuel Utilization," *ECS Transactions*, Vol. 91, No. 1, 2019, p. 801. https://doi.org/10.1149/09101.0801ecst

[66] Tucker, D., Abreu-Sepulveda, M., and Harun, N. F., "SOFC Lifetime Assessment in Gas Turbine Hybrid Power Systems," *Journal of Fuel Cell Science and Technology*, Vol. 11, No. 5, 2014, Paper 051008. https://doi.org/10.1115/1.4028158

[67] Staffell, I., Ingram, A., and Kendall, K., "Energy and Carbon Payback Times for Solid Oxide Fuel Cell Based Domestic CHP," *International Journal of Hydrogen Energy*, Vol. 37, No. 3, 2012, pp. 2509–2523. https://doi.org/10.1016/j.ijhydene.2011.10.060

[68] Lanzini, A., Madi, H., Chiodo, V., Papurello, D., Maisano, S., Santarelli, M., and Herle, J. V., "Dealing with Fuel Contaminants in Biogas-Fed Solid Oxide Fuel Cell (SOFC) and Molten Carbonate Fuel Cell (MCFC) Plants: Degradation of Catalytic and Electro-Catalytic Active Surfaces and Related Gas Purification Methods," *Progress in Energy and Combustion Science*, Vol. 61, No. 7, 2017, pp. 150–188. https://doi.org/10.1016/j.pecs.2017.04.002

[69] Mougin, J., Ravel, S., de Vito, E., and Petijean, M., "Influence of Fuel Contaminants on SOFC Operation: Effect on Performance and Degradation Mechanisms," *Electrochemical Society Transactions*, Vol. 7, No. 1, 2007, p. 459. https://doi.org/10.1149/1.2729124

[70] Fragiacomo, P., Piraino, F., Genovese, M., Corigliano, O., and De Lorenzo, G., "Experimental Activities on a Hydrogen-Powered Solid Oxide Fuel Cell System and Guidelines for Its Implementation in Aviation and Maritime Sectors," *Energies*, Vol. 16, No. 15, 2023, Paper 5671. https://doi.org/10.3390/en16155671

[71] Mendonça, C., Ferreira, A., and Santos, D. M. F., "Towards the Commercialization of Solid Oxide Fuel Cells: Recent Advances in Materials and Integration Strategies," *Fuels*, Vol. 2, No. 4, 2021, pp. 393–419. https://doi.org/10.3390/fuels2040023

[72] Zeng, Z., Qian, Y., Zhang, Y., Hao, C., Dan, D., and Zhuge, W., "A Review of Heat Transfer and Thermal Management Methods for Temperature Gradient Reduction in Solid Oxide Fuel Cell (SOFC) Stacks," *Applied Energy*, Vol. 280, No. 12, 2020, Paper 115899. https://doi.org/10.1016/j.apenergy.2020.115899

[73] Sanz-Morère, I., Eastham, S. D., Speth, R. L., and Barrett, S. R. H., "Reducing Uncertainty in Contrail Radiative Forcing Resulting from Uncertainty in Ice Crystal Properties," *Environmental Science & Technology Letters*, Vol. 7, No. 6, 2020, pp. 371–375. https://doi.org/10.1021/acs.estlett.0c00150